



HAL
open science

Discovery of a dormant 33 solar-mass black hole in pre-release Gaia astrometry

P. Panuzzo, T. Mazeh, F. Arenou, B. Holl, E. Caffau, A. Jorissen, C. Babusiaux, P. Gavras, J. Sahlmann, U. Bastian, et al.

► **To cite this version:**

P. Panuzzo, T. Mazeh, F. Arenou, B. Holl, E. Caffau, et al.. Discovery of a dormant 33 solar-mass black hole in pre-release Gaia astrometry. *Astronomy and Astrophysics - A&A*, 2024, 686, pp.L2. 10.1051/0004-6361/202449763 . hal-04589888

HAL Id: hal-04589888

<https://hal.science/hal-04589888>

Submitted on 27 May 2024

HAL is a multi-disciplinary open access archive for the deposit and dissemination of scientific research documents, whether they are published or not. The documents may come from teaching and research institutions in France or abroad, or from public or private research centers.

L'archive ouverte pluridisciplinaire **HAL**, est destinée au dépôt et à la diffusion de documents scientifiques de niveau recherche, publiés ou non, émanant des établissements d'enseignement et de recherche français ou étrangers, des laboratoires publics ou privés.

LETTER TO THE EDITOR

Discovery of a dormant 33 solar-mass black hole in pre-release *Gaia* astrometry^{*}

Gaia Collaboration: P. Panuzzo¹, T. Mazeh², F. Arenou¹, B. Holl^{3,4}, E. Caffau¹, A. Jorissen⁵, C. Babusiaux⁶, P. Gavras⁷, J. Sahlmann⁷, U. Bastian⁸, Ł. Wyrzykowski⁹, L. Eyer³, N. Leclerc¹, N. Bauchet¹, A. Bombrun¹⁰, N. Mowlavi³, G. M. Seabroke¹¹, D. Teyssier¹², E. Balbinot^{13,14}, A. Helmi¹³, A. G. A. Brown¹⁴, A. Vallenari¹⁵, T. Prusti¹⁶, J. H. J. de Bruijne¹⁶, A. Barbier¹⁷, M. Biermann⁸, O. L. Creevey¹⁸, C. Ducourant¹⁹, D. W. Evans²⁰, R. Guerra²¹, A. Hutton²², C. Jordi^{23,24}, S. A. Klioner²⁵, U. Lammers²¹, L. Lindegren²⁶, X. Luri^{23,27,24}, F. Mignard¹⁸, C. Nicolas¹⁷, S. Randich²⁸, P. Sartoretti¹, R. Smiljanic²⁹, P. Tanga¹⁸, N. A. Walton²⁰, C. Aerts^{30,31,32}, C. A. L. Bailer-Jones³², M. Cropper¹¹, R. Drimmel³³, F. Jansen³⁴, D. Katz¹, M. G. Lattanzi^{33,35}, C. Soubiran¹⁹, F. Thévenin¹⁸, F. van Leeuwen²⁰, R. Andrae³², M. Audard³, J. Bakker²¹, R. Blomme³⁶, J. Castañeda^{37,23,24}, F. De Angeli²⁰, C. Fabricius^{24,23,27}, M. Fouesneau³², Y. Frémat³⁶, L. Galluccio¹⁸, A. Guerrier¹⁷, U. Heiter³⁸, E. Masana^{24,23,27}, R. Messineo³⁹, K. Nienartowicz^{40,4}, F. Pailler¹⁷, F. Riclet¹⁷, W. Roux¹⁷, R. Sordo¹⁵, G. Gracia-Abril^{41,8}, J. Portell^{23,27,24}, M. Altmann^{8,42}, K. Benson¹¹, J. Berthier⁴³, P. W. Burgess²⁰, D. Busonero³³, G. Busso²⁰, C. Cacciari⁴⁴, H. Cánovas¹², J. M. Carrasco^{24,23,27}, B. Carry¹⁸, A. Cellino³³, N. Cheek⁴⁵, G. Clementini⁴⁴, Y. Damerdjji^{46,47}, M. Davidson⁴⁷, P. de Teodoro²¹, L. Delchambre⁴⁶, A. Dell’Oro²⁸, E. Fraile Garcia⁷, D. Garabato⁴⁹, P. García-Lario²¹, R. Haigron¹, N. C. Hambly⁴⁷, D. L. Harrison^{20,50}, D. Hatzidimitriou⁵¹, J. Hernández²¹, D. Hestroffer⁴³, S. T. Hodgkin²⁰, S. Jamal³², G. Jevardat de Fombelle³, S. Jordan⁸, A. Krone-Martins^{52,53}, A. C. Lanzafame^{54,55}, W. Löffler⁸, A. Lorca²², O. Marchal⁵⁶, P. M. Marrese^{57,58}, A. Moitinho⁵³, K. Muinonen^{59,60}, M. Nuñez Campos²², I. Oreshina-Slezak¹⁸, P. Osborne²⁰, E. Pancino^{28,58}, T. Pauwels³⁶, A. Recio-Blanco¹⁸, M. Riello²⁰, L. Rimoldini⁴, A. C. Robin⁶¹, T. Roegiers⁶², L. M. Sarro⁶³, M. Schultheis¹⁸, M. Smith¹¹, A. Sozzetti³³, E. Utrilla²², M. van Leeuwen²⁰, K. Weingrill⁶⁴, U. Abbas³³, P. Abraham^{65,66,67}, A. Abreu Aramburu⁶⁸, S. Ahmed²⁰, G. Altavilla^{57,58}, M. A. Álvarez⁴⁹, F. Anders^{23,27,24}, R. I. Anderson⁶⁹, E. Anglada Varela²², T. Antoja^{23,27,24}, S. Baig⁷⁰, D. Baines⁷¹, S. G. Baker¹¹, L. Balaguer-Núñez^{24,23,27}, Z. Balog^{8,32}, C. Barache⁴², M. Barros⁷², M. A. Barstow⁷³, S. Bartolomé^{24,23,27}, D. Bashi^{2,74}, J.-L. Bassilana⁷⁵, N. Baudeau⁷⁶, U. Becciani⁵⁴, L. R. Bedin¹⁵, I. Bellas-Velidis⁷⁷, M. Bellazzini⁴⁴, W. Beordo^{33,35}, M. Bernet^{23,27,24}, C. Bertolotto³⁹, S. Bertone^{33,78}, L. Bianchi⁷⁹, A. Binnenfeld⁸⁰, S. Blanco-Cuaresma^{81,82}, J. Bland-Hawthorn^{83,84}, A. Blazere⁸⁵, T. Boch⁵⁶, D. Bossini^{86,15}, S. Bouquillon^{42,87}, A. Bragaglia⁴⁴, J. Braine¹⁹, E. Bratsolis⁸⁸, E. Breedt²⁰, A. Bressan⁸⁹, N. Brouillet¹⁹, E. Brugaletta⁵⁴, B. Bucciarelli^{33,35}, A. G. Butkevich³³, R. Buzzzi³³, A. Camut⁹⁰, R. Cancelliere⁹¹, T. Cantat-Gaudin³², D. Capilla Guilarte²⁰, R. Carballo⁹², T. Carlucci⁴², M. I. Carnerero³³, J. Carretero^{93,94,95}, S. Carton⁷⁵, L. Casamiquela¹, A. Casey⁹⁶, M. Castellani⁵⁷, A. Castro-Ginard¹⁴, L. Ceraj⁹⁷, V. Cesare⁵⁴, P. Charlot¹⁹, C. Chaudet⁴, L. Chemin⁹⁸, A. Chiavassa¹⁸, N. Chornay⁴, D. Chosson⁹⁹, W. J. Cooper^{70,33}, T. Cornez⁷⁵, S. Cowell²⁰, M. Crosta^{33,100}, C. Crowley¹⁰, M. Cruz Reyes⁶⁹, C. Dafonte⁴⁹, M. Dal Ponte¹⁵, M. David¹⁰¹, P. de Laverny¹⁸, F. De Luise¹⁰², R. De March³⁹, A. de Torres¹⁰, E. F. del Peloso⁸, M. Delbo¹⁸, A. Delgado⁷, J.-B. Delisle³, C. Demouchy¹⁰³, E. Denis^{18,104}, T. E. Dharmawardena¹⁰⁵, F. Di Giacomo¹⁰², C. Diener²⁰, E. Distefano⁵⁴, C. Dolding¹¹, K. Dsilva⁵, H. Enke⁶⁴, C. Fabre⁸⁵, M. Fabrizio^{57,58}, S. Faigler², M. Fatović⁹⁷, G. Fedorets^{106,59,107}, J. Fernández-Hernández⁷, P. Fernique⁵⁶, F. Figueras^{23,27,24}, C. Fouron⁷⁶, F. Fragkoudi¹⁰⁸, M. Gai³³, M. Galinier¹⁸, A. Garcia-Serrano^{24,23,27}, M. García-Torres¹⁰⁹, A. Garofalo⁴⁴, E. Gerlach²⁵, R. Geyer²⁵, P. Giacobbe³³, G. Gilmore^{20,110}, S. Girona¹¹¹, G. Giuffrida⁵⁷, A. Gomboc¹¹², A. Gomez⁴⁹, I. González-Santamaría⁴⁹, E. Gosset^{46,113}, M. Granvik^{59,114}, V. Gregori Barrera^{24,23,27}, R. Gutiérrez-Sánchez¹², M. Haywood¹, A. Helmer⁷⁵, S. L. Hidalgo^{115,116}, T. Hilger²⁵, D. Hobbs²⁶, C. Hottier¹, H. E. Huckle¹¹, Ó. Jiménez-Arranz^{23,27,24}, J. Juaristi Campillo⁸, Z. Kaczmarek⁸, P. Kervella⁹⁹, S. Khanna^{33,13}, M. Kontizas⁵¹, G. Kordopatis¹⁸, A. J. Korn³⁸, Á. Kóspál^{65,32,66}, Z. Kostrzewa-Rutkowska^{68,14}, K. Kruszyńska¹¹⁷, M. Kun⁶⁵,

S. Lambert⁴², A. F. Lanza⁵⁴, Y. Lebreton^{99,118}, T. Lebzelter⁶⁷, S. Leccia¹¹⁹, G. Lecoutre⁶¹, S. Liao^{120,33,121}, L. Liberato^{18,122}, E. Licata³³, E. Livanou⁵¹, A. Lobel³⁶, J. López-Miralles²², C. Loup⁵⁶, M. Madarász⁶⁵, L. Mahy³⁶, R. G. Mann⁴⁷, M. Manteiga¹²³, C. P. Marcellino⁵⁴, J. M. Marchant¹²⁴, M. Marconi¹¹⁹, D. Marín Pina^{23,27,24}, S. Marinoni^{57,58}, D. J. Marshall¹²⁵, J. Martín Lozano⁴⁵, L. Martín Polo¹²⁶, J. M. Martín-Fleitas²², G. Marton⁶⁵, D. Mascarenhas⁷⁵, A. Masip^{24,23,27}, A. Mastrobuono-Battisti¹, P. J. McMillan⁷³, J. Meichsner²⁵, J. Merc¹²⁷, S. Messina⁵⁴, N. R. Millar²⁰, A. Mints⁶⁴, D. Mohamed⁹⁰, D. Molina^{27,23,24}, R. Molinaro¹¹⁹, L. Molnár^{65,66}, M. Monguió^{23,128}, P. Montegriffo⁴⁴, L. Monti⁴⁴, A. Mora²², R. Morbidelli³³, D. Morris⁴⁷, R. Mudimadugula⁶⁴, T. Muraveva⁴⁴, I. Musella¹¹⁹, Z. Nagy⁶⁵, N. Nardetto¹⁸, C. Navarrete¹⁸, S. Oh^{20,129}, C. Ordenovic¹⁸, O. Orenstein², C. Pagani⁷³, I. Pagano⁵⁴, L. Palaversa⁹⁷, P. A. Palicio¹⁸, L. Pallas-Quintela⁴⁹, M. Pawlak^{130,26}, A. Penttilä⁵⁹, P. Pesciullesi⁷, M. Pinamonti³³, E. Plachy^{65,66}, L. Planquart⁵, G. Plum¹, E. Poggio^{33,18}, D. Pourbaix^{5,113,†}, A. M. Price-Whelan¹³¹, L. Pulone⁵⁷, V. Rabin⁴³, M. Rainer^{132,28}, C. M. Raiteri³³, P. Ramos^{133,23,24}, M. Ramos-Lerate¹², M. Ratajczak⁹, P. Re Fiorentin³³, S. Regibo³⁰, C. Reylé⁶¹, V. Ripepi¹¹⁹, A. Riva³³, H.-W. Rix³², G. Rixon²⁰, G. Robert⁷⁵, N. Robichon¹, C. Robin⁷⁵, M. Romero-Gómez^{23,27,24}, N. Rowell⁴⁷, D. Ruz Mieres²⁰, K. A. Rybicki¹³⁴, G. Sadowski⁵, A. Sagristà Sellés⁸, N. Sanna²⁸, R. Santoveña⁴⁹, M. Sarasso³³, M. H. Sarmiento²², C. Sarrate Riera^{37,23,24}, E. Sciacca⁵⁴, D. Ségransan³, M. Semczuk^{23,27,24}, S. Shahaf¹³⁴, A. Siebert^{56,135}, E. Slezak¹⁸, R. L. Smart^{33,70}, O. N. Snaith^{1,136}, E. Solano¹³⁷, F. Solitro³⁹, D. Souami^{99,138}, J. Souchay⁴², E. Spitoni^{18,139}, F. Spoto⁸¹, L. A. Squillante³⁹, I. A. Steele¹²⁴, H. Steidelmüller²⁵, J. Surdej⁴⁶, L. Szabados⁶⁵, F. Taris⁴², M. B. Taylor¹⁴⁰, R. Teixeira¹⁴¹, T. Tepper-García^{83,84}, W. Thuillot⁴³, L. Tolomei³⁹, N. Tonello¹¹¹, F. Torra^{23,27,24}, G. Torralba Elipe^{49,142,143}, M. Trabucchi^{86,3}, E. Trentin^{144,64}, M. Tsantaki²⁸, C. Turon¹, A. Ulla^{145,146}, N. Unger³, I. Valtchanov¹², O. Vanel¹, A. Vecchiato³³, D. Vicente¹¹¹, E. Villar^{37,23,24}, M. Weiler^{24,23,27}, H. Zhao^{18,147}, J. Zorec¹⁴⁸, S. Zucker^{80,2}, A. Župić⁴⁹ and T. Zwitter¹⁴⁹

(Affiliations can be found after the references)

Received 27 February 2024 / Accepted 30 March 2024

ABSTRACT

Context. Gravitational waves from black-hole (BH) merging events have revealed a population of extra-galactic BHs residing in short-period binaries with masses that are higher than expected based on most stellar evolution models – and also higher than known stellar-origin black holes in our Galaxy. It has been proposed that those high-mass BHs are the remnants of massive metal-poor stars.

Aims. *Gaia* astrometry is expected to uncover many Galactic wide-binary systems containing dormant BHs, which may not have been detected before. The study of this population will provide new information on the BH-mass distribution in binaries and shed light on their formation mechanisms and progenitors.

Methods. As part of the validation efforts in preparation for the fourth *Gaia* data release (DR4), we analysed the preliminary astrometric binary solutions, obtained by the *Gaia* Non-Single Star pipeline, to verify their significance and to minimise false-detection rates in high-mass-function orbital solutions.

Results. The astrometric binary solution of one source, *Gaia* BH3, implies the presence of a $32.70 \pm 0.82 M_{\odot}$ BH in a binary system with a period of 11.6 yr. *Gaia* radial velocities independently validate the astrometric orbit. Broad-band photometric and spectroscopic data show that the visible component is an old, very metal-poor giant of the Galactic halo, at a distance of 590 pc.

Conclusions. The BH in the *Gaia* BH3 system is more massive than any other Galactic stellar-origin BH known thus far. The low metallicity of the star companion supports the scenario that metal-poor massive stars are progenitors of the high-mass BHs detected by gravitational-wave telescopes. The Galactic orbit of the system and its metallicity indicate that it might belong to the Sequoia halo substructure. Alternatively, and more plausibly, it could belong to the ED-2 stream, which likely originated from a globular cluster that had been disrupted by the Milky Way.

Key words. astrometry – binaries: spectroscopic – stars: black holes – stars: evolution – stars: massive – stars: Population II

1. Introduction

Since the first event detected in 2015 (Abbott et al. 2016) by the LIGO/Virgo collaboration, the detection of black-hole (BH) mergers via gravitational waves has uncovered the existence of a population of BHs residing in short-period binaries with masses higher than $30 M_{\odot}$, ranging up to $85 M_{\odot}$ (Abbott et al. 2020b, 2021).

Stellar evolution models have difficulties in explaining such large masses for BHs of stellar origin: stars with an initial mass larger than $30 M_{\odot}$ are predicted to lose most of their mass during their evolution, due to the onset of strong winds, producing BHs with masses below $20 M_{\odot}$ (Vink 2008; Belczynski et al. 2007; Sukhbold et al. 2016).

The masses of the merging BHs detected via gravitational waves are also larger than any known stellar-origin BHs in our Galaxy: all confirmed or candidate BHs of stellar origin in the Milky Way have typical masses around or below $10 M_{\odot}$, with Cyg X-1 ($\sim 20 M_{\odot}$, Miller-Jones et al. 2021) being the most massive one known thus far. However, the known stellar-origin BHs,

* Full Table B.1 and Table B.2 with *Gaia* epoch data are available at the CDS via anonymous ftp to cdsarc.cds.unistra.fr (130.79.128.5) or via <https://cdsarc.cds.unistra.fr/viz-bin/cat/J/A+A/686/L2>

** NASA Hubble Fellow.

† Deceased.

Table 1. Basic properties of *Gaia* BH3 from the *Gaia* DR3 catalogue.

Parameter	Value
α [deg]	294.8278625082 ^(a)
σ_{α^*} [mas]	0.051
δ [deg]	14.9309796086 ^(a)
σ_{δ} [mas]	0.052
ϖ [mas]	1.679 ± 0.069 ^(b)
μ_{α}^* [mas yr ⁻¹]	-22.235 ± 0.062
μ_{δ} [mas yr ⁻¹]	-155.276 ± 0.059
G [mag]	11.2311 ± 0.0028
$G_{BP} - G_{RP}$ [mag]	1.2156 ± 0.0048
G_{RVS} [mag]	10.2289 ± 0.0122
T_{eff} [K]	5340^{+212}_{-198}
$\log g$	$3.08^{+0.36}_{-0.30}$
[M/H]	$-2.76^{+0.19}_{-0.09}$
[α /Fe]	0.54 ± 0.06
RV [km s ⁻¹]	-333.2 ± 3.4

Notes. Astrophysical parameters are from GSP-Spec ANN. ^(a)The reference epoch of DR3 coordinates is J2016.0 (JD 2457389.0). ^(b)A zero-point correction (Lindgren et al. 2021a) of 35.4 μ as has been applied to the parallax value given in the catalogue.

mainly limited to short-period X-ray binaries, are only a very tiny fraction of the expected number of BHs in our Galaxy ($\sim 10^8$ e.g. Olejak et al. 2020). In fact, stellar-origin BHs are hard to detect because most of them do not interact with a companion. So, the lack of data on BHs with masses larger than $20 M_{\odot}$ could be due to an observational bias. Indirect methods such as gravitational microlensing have also yielded only one robust discovery of a single BH with mass, of about $7 M_{\odot}$ (Lam et al. 2022; Sahu et al. 2022).

The detection of mergers of BHs with masses larger than $30 M_{\odot}$ can be reconciled with stellar evolution models if the progenitors of the high-mass BHs are low-metallicity stars (Mapelli et al. 2009; Belczynski et al. 2010a, 2016; Ziosi et al. 2014; Fryer et al. 2012). The lack of metals substantially decreases the mass loss during the stellar lifetime (Vink 2008) and reduces the radius of the evolving progenitors (Hurley et al. 2000; Belczynski et al. 2010a), the latter effect decreasing the probability of merging during the common-envelope phase (Belczynski et al. 2007) in binary systems. Finally, the higher mass of the BHs produced by low-metallicity progenitors is expected to decrease substantially or eliminate the natal kick strength at the birth of the BHs, preserving the binary as a bound system (Belczynski et al. 2010b). The maximum metallicity for the formation of the high-mass BHs is a matter of active debate, with some models predicting the formation of $30 M_{\odot}$ BHs even at solar metallicities (Bavera et al. 2023).

Since its Data Release 3 (DR3, Gaia Collaboration 2023b), the *Gaia* mission (Gaia Collaboration 2016) has increased the number of detected stellar binary systems by two orders of magnitude (Gaia Collaboration 2023a; Halbwegs et al. 2023; Gosset et al. 2024) This has opened up the possibility of detecting BHs in binary systems that do not interact with their companion (see also Giesers et al. 2018; Saracino et al. 2022). Moreover, the ability of *Gaia* to measure the astrometric orbit of such systems allows the measurement of the inclination of the orbit, providing a robust estimate of the mass of the dark companion. Two dormant BHs, *Gaia* BH1 and BH2 (El-Badry et al. 2023a,b; Tanikawa et al. 2023; Chakrabarti et al. 2023) were discovered in *Gaia* binaries of DR3. *Gaia* Data Release 4 (DR4) is expected

to contain a larger number of binary systems than *Gaia* DR3; consequently, this will provide a greater number of BH-hosting systems, which will help to shed light on the BH population and the mechanisms in action in the BHs' formation.

In this Letter, we report the serendipitous discovery of a nearby (~ 590 pc) binary system composed of an old, very metal-poor¹, giant star orbiting a BH in 11.6 yr. The estimated BH mass, $33 M_{\odot}$, is substantially higher than all known Galactic BHs and is in the mass range of the extra-galactic BHs detected by gravitational waves.

The system was identified while validating the preliminary *Gaia* astrometric binary solutions produced in preparation for DR4 and subsequently confirmed by *Gaia* RVS radial-velocity data. We took the exceptional step of the publication of this paper based on preliminary data ahead of the official DR4 due to the unique nature of the discovery, which we believe should not be kept from the scientific community until the next release. An early disclosure will also enable an early and extensive follow-up by the community.

2. Observations and analysis

2.1. Properties of the source

Gaia DR3 4318465066420528000 (also known as LS II +14 13 and 2MASS J19391872+1455542), hereafter denoted as *Gaia* BH3, is a bright source in the constellation Aquila, known to be a high proper-motion star (Lépine & Shara 2005). Its basic properties from the *Gaia* DR3 archive are reported in Table 1. Its absolute magnitude and color (Riello et al. 2021; Sartoretti et al. 2023) identify it as a star climbing the giant branch (see Fig. 1). The source was analysed by the Astrophysical Parameters Inference System (Apsis, Creevey et al. 2023; Fouesneau et al. 2023). It has been identified as a G spectral-type star by the ESP-ELS algorithm (Sect. 11.3.7 of the online documentation, Ulla et al. 2022) and the GSP-Spec ANN parameters (Recio-Blanco et al. 2023) indicate it as a metal-poor giant. No GSP-Phot result (Andrae et al. 2023) is published in the *Gaia* archive, while the parameters provided by GSP-Spec MatisseGauguin (Recio-Blanco et al. 2023) carry large uncertainties.

The source is not known as a variable star in the literature, neither in the AAVSO International Database, nor in the ASAS-SN database. We inspected ASAS-SN, ZTF, and TESS photometry, finding that the source does not present any significant periodic variability. The source was not observed with *XMM-Newton*, *Chandra* nor GALEX, nor it is present in the RAVE, APOGEE, LAMOST, or GALAH spectroscopic surveys. No eROSITA data have been made available yet for *Gaia* BH3, which belongs to the eastern Galactic hemisphere.

2.2. Astrometry and orbital solution

The system was identified while validating astrometric binaries orbital solutions produced by the Non-Single Star (NSS) pipeline in a preliminary run (identified as NSS 4.1), done in preparation of *Gaia* DR4. The NSS pipeline used in the NSS 4.1 run is similar to the one used in the *Gaia* DR3, which is described in Halbwegs et al. (2023) and in Sect. 7.2.2 of the DR3 NSS documentation (Pourbaix et al. 2022), with improvements in the filtering of spurious solutions. The NSS pipeline processed astrometric data produced by preliminary runs of the Intermediate

¹ We use the nomenclature from Beers & Christlieb (2005) where very metal-poor are those stars having [Fe/H] < -2.

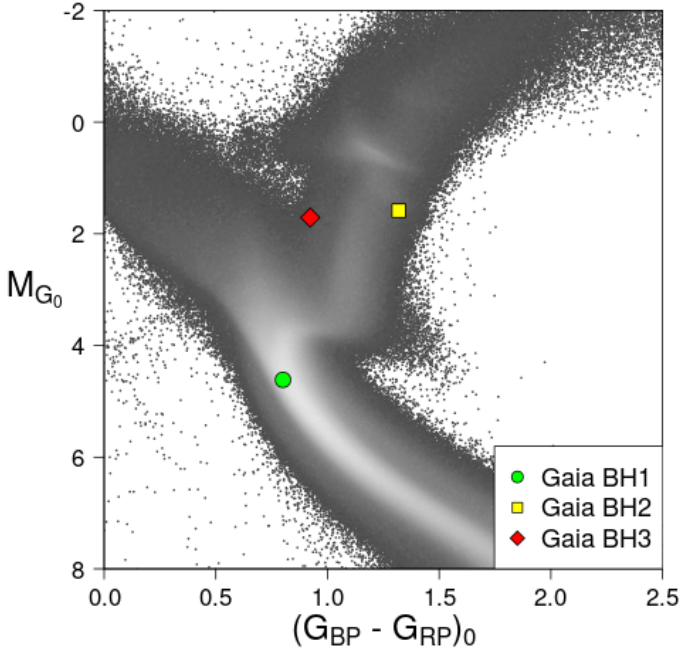


Fig. 1. *Gaia* BH3 position in the *Gaia* color-magnitude diagram, compared with the position of *Gaia* BH1, BH2 and the low extinction ($A_0 < 0.05$ mag) *Gaia* DR3 color-magnitude diagram. All extinctions are estimated through the Lallement et al. (2022) extinction map.

Data Update (IDU; see Fabricius et al. 2016) and the Astrometric Global Iterative Solution (AGIS; see Lindegren et al. 2021b) pipelines, covering the time range from JD 2456941.6218 to JD 2458869.4177 (TCB²), for a total of about 64 months. The NSS 4.1 run was executed on an input list of 10.4 million sources, chosen to be brighter than $G_{RVS} = 14$ mag, and produced almost 1.5 million orbital solutions. We note that the final NSS run for DR4 will extend to fainter magnitudes, and it is expected to produce a much larger number of binary solutions. Further details on the NSS 4.1 run can be found in Appendix A.

For each orbital solution, we computed the astrometric mass function from the angular semi-major axis of the photocentre orbit (a_0), period (P), and parallax (ϖ) as:

$$f_M = (a_0/\varpi)^3 (1 \text{ yr}/P)^2 M_\odot. \quad (1)$$

For an astrometric binary, the mass function depends on the masses of the components (M_1 , M_2) and on their flux ratio, $\mathcal{F}_2/\mathcal{F}_1$ (Halbwachs et al. 2023). For an invisible companion ($\mathcal{F}_2/\mathcal{F}_1 = 0$) the mass function simplifies to:

$$f_M = M_2 \left(\frac{M_2}{M_1 + M_2} \right)^2, \quad (2)$$

from which it follows that $M_2 \geq f_M$. Given f_M and an estimate of the mass of the visible component (M_1), Eq. (2) can be used to solve for the mass of the dark companion (M_2).

Among the 1.5 million orbital solutions, *Gaia* BH3 yielded the largest mass function, $32.03 \pm 0.64 M_\odot$, with a significance (a_0/σ_{a_0}) of 48.1; no other solution has a mass function larger than $20 M_\odot$. In Fig. 2, we show the orbital solution and the residuals, from which the strength of the astrometric signal of the orbit, along with the robustness and quality of the solution can

be appreciated. The Campbell orbital elements of the source are reported in the central column of Table 2. We note that the NSS pipeline used in this preliminary run produces Thiele-Innes elements; the Campbell elements and their uncertainties were computed using the equations in Appendix A of Halbwachs et al. (2023). The astrometric mass function value and its uncertainty were computed using Monte Carlo resampling of the Thiele-Innes elements, the parallax and the period, in order to take into account the correlations between parameters; in particular, between a_0 and the period. To make sure this procedure would yield reliable results, we first checked that the correlations are sufficiently well behaved to allow for Monte Carlo resampling, following Sect. 6.1 of Babusiaux et al. (2023).

A word of caution is necessary on the parallax value, and thus on the astrometric mass function: as in previous releases, the *Gaia* parallaxes are affected by a small bias (see Lindegren et al. 2021a), but we do not have enough information at this stage to quantify the bias for the preliminary NSS solutions. As a consequence, the uncertainty on the mass function reported in Table 2 is underestimated.

2.3. Spectroscopy and combined orbital solution

The *Gaia* RVS (Cropper et al. 2018) data of sources with an orbital solution from the NSS 4.1 run were processed with the DR4 operational RVS pipeline. Improvements with respect to the DR3 version will be described in the *Gaia* DR4 documentation; the DR3 RVS pipeline is described in Sartoretti et al. (2018), Katz et al. (2023), and Sartoretti et al. (2022). It is worth mentioning that the DR4 RVS pipeline includes the correction for the effect of the astrometric orbital motion, discussed in Holl et al. (2023); in particular, Sect. 3.3.1. The DR4 RVS data cover the time range from JD 2456863.9385 to JD 2458869.4177, namely, about 67 months. The pipeline produced 17 valid epoch radial velocities for *Gaia* BH3, reported in Appendix B, using a template spectrum with $T_{\text{eff}} = 6000$ K, $\log g = 3.5$ and $[\text{Fe}/\text{H}] = -1.5$ (see Blomme et al. 2017). The template parameters were estimated by the pipeline from the RVS spectrum itself.

We used the DR3 NSS pipeline code to compute an orbital solution combining astrometric data and *Gaia* RVS radial velocities (`nss_solution_type = AstroSpectroSB1`). The details of the adopted model are described in Sect. 7.7.3 of Pourbaix et al. (2022). We recall that in the combined solution model only the period, eccentricity, and periastron time are in common between the astrometric and the spectroscopic part of the solution. There is no constraint to impose that the semi-major axis of the photocentre orbit in AU ($= a_0/\varpi$) would be equal to the semi-major axis of the spectroscopic orbit a_1 , as expected in the case of a dark companion. The consistency between a_0 and a_1 allows us to check whether the flux ratio is indeed compatible with a value of zero.

As discussed in Sect. 2.2, the parallax derived by the NSS pipeline for the combined solution ($\varpi = 1.6808 \pm 0.0086$ mas) is affected by a bias which we cannot quantify. In order to avoid its effect on the mass function, we estimate the latter using a_1 instead of a_0/ϖ , namely:

$$f_M = \left(\frac{a_1}{1 \text{ AU}} \right)^3 \left(\frac{1 \text{ yr}}{P} \right)^2 M_\odot, \quad (3)$$

resulting in a value of $31.23 \pm 0.81 M_\odot$. Assuming the equality between the photocentre and the spectroscopic orbit, we can also provide an alternative estimation of the parallax as

$$\varpi = a_0/a_1, \quad (4)$$

² TCB: Barycentric Coordinate Time, the time scale used here for all *Gaia* dates.

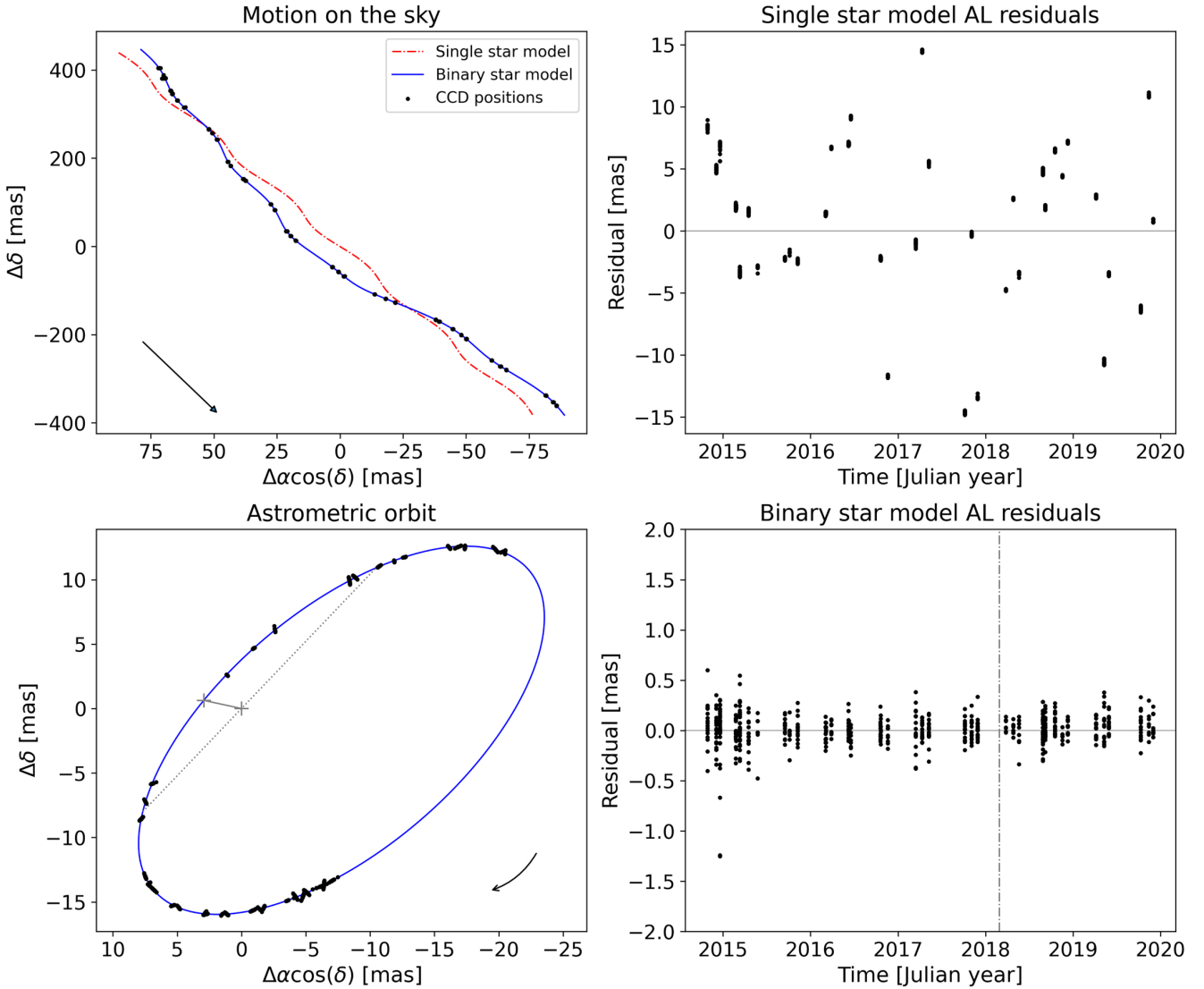


Fig. 2. Astrometric data of *Gaia* BH3. Top-left panel: Motion on the sky of the photocentre of the source, as seen by *Gaia* in the different CCD transits (dots), compared with the best fitting single-star solution from AGIS and the astrometric-binary solution from the NSS pipeline; the arrow indicates the direction of the proper motion. Bottom-left panel: Derived astrometric orbit of the photocentre, after a subtraction of parallax and proper motion, compared with the astrometric measurements. We note that only one-dimensional (1D) along-scan (AL) astrometry was used by the NSS pipeline. The position of the photocentre on the sky corresponding to each measurement is derived combining the measured one-dimensional AL position and the assumed orbital solution. The + signs show the barycentre and the position of the periastron, the dotted line shows the line of nodes, and the arrow indicates the direction of the motion along the orbit. In the top-right and bottom-right panels, we can see the residuals of the along-scan (AL) astrometric measurements for, respectively, the single-star solution and the binary-star solution. The vertical dot-dashed line in the bottom-right panel marks the time of the periastron passage.

which results in a value of 1.6933 ± 0.0164 mas.

The Campbell orbital elements of the combined solution for *Gaia* BH3 are reported in Table 2. The combined solution is very similar to the astrometric solution, with slightly smaller uncertainties, and a better goodness-of-fit (GoF, in the HIPPARCOS sense, see Pourbaix et al. 2022), as a result of a stronger filtering of outliers. Radial velocities predicted by the combined solution are compared with the measurements in Fig. 3. In Fig. 4, we show the combined and normalised RVS spectrum (see Seabroke et al. in prep.) compared with the template spectrum.

Given the extreme value of the mass function of the system and the importance of its detection, a confirmation with ground-based observations was indispensable to discard the possibility of a spurious solution. We thus observed *Gaia* BH3 with the HERMES spectrograph (Raskin et al. 2011) mounted

on the 1.2-m *Mercator* telescope at the Roque de los Muchachos Observatory (Spain), and with the SOPHIE spectrograph (Perruchot et al. 2008) mounted on the 1.93-m telescope of the Observatoire de Haute-Provence (France). A search in the ESO archive revealed that the source was observed with the UVES spectrograph (Dekker et al. 2000) mounted on the VLT. Details on the data reduction of these observations can be found in Appendix C. The spectra do not show any sign of the presence of a second component, nor of continuum filling of absorption lines; furthermore, no emission line was detected. Radial velocities were derived for each ground-based observation and their values are reported in Table C.1. Although these values were not used to derive the orbital solution described above, they are in agreement with the predicted radial velocity within 0.5 km s^{-1} ; this is less than the uncertainty of the orbital solution, as can be

Table 2. Campbell orbital elements of the *Gaia* BH3 system and the astrometric parameters of its barycentre.

Parameter	Astrometric solution	Combined solution
α [deg]	294.8278502411 ^(a)	294.8278502301 ^(a)
σ_{α^*} [mas]	0.060	0.054
δ [deg]	14.9309190720 ^(a)	14.9309190869 ^(a)
σ_{δ} [mas]	0.086	0.074
ϖ [mas]	1.6747 ± 0.0094	1.6933 ± 0.0164 ^(b)
μ_{α}^* [mas yr ⁻¹]	-28.372 ± 0.077	-28.317 ± 0.067
μ_{δ} [mas yr ⁻¹]	-155.150 ± 0.129	-155.221 ± 0.111
P [days]	4194.7 ± 112.3	4253.1 ± 98.5
e	0.7262 ± 0.0056	0.7291 ± 0.0048
a_0 [mas]	27.07 ± 0.56	27.39 ± 0.49
i [deg]	110.659 ± 0.107	110.580 ± 0.095
T_p [JD, TCB]	2458177.28 ± 0.98	2458177.39 ± 0.88
Ω [deg]	136.200 ± 0.147	136.236 ± 0.128
ω [deg]	77.77 ± 0.66	77.34 ± 0.76
a_1 [AU]	...	16.17 ± 0.27
γ [km s ⁻¹]	...	-357.31 ± 0.44
f_M [M_{\odot}]	32.03 ± 0.64	31.23 ± 0.81
GoF	2.17	-0.53

Notes. ^(a)The reference epoch of DR4 coordinates is J2017.5 (JD 2457936.875). ^(b)Derived as a_0/a_1 , see text.

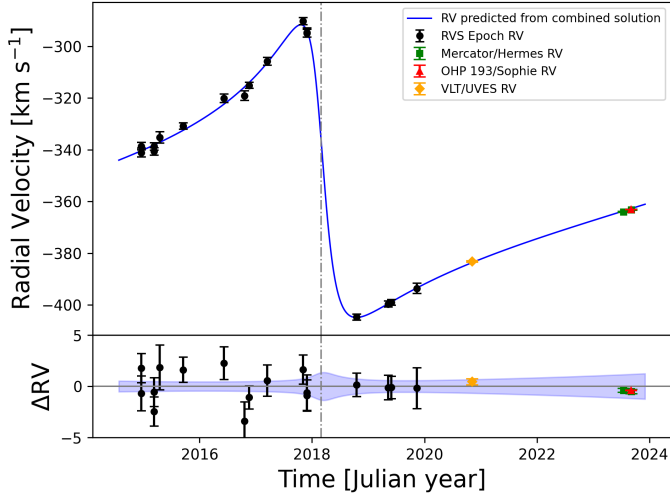


Fig. 3. Radial-velocity evolution of *Gaia* BH3. Top panel: Comparison between the radial-velocity evolution predicted from the combined *Gaia* astrometric-spectroscopic binary model (blue solid line) and the epoch radial velocities measured with the *Gaia* RVS instrument (black filled circles), and ground-based measurements for *Gaia* BH3. Bottom panel: Radial-velocity residuals with respect to the binary solution compared with the 1- σ uncertainty of the predicted radial-velocity evolution (blue shaded area). The vertical dot-dashed line in both panels marks the time of the periastron passage.

seen in Fig. 3. This result confirms the reality and accuracy of the orbital solution derived from *Gaia* data.

2.4. Stellar parameters, abundances and Galactic orbit

We derived new stellar parameters of the luminous component, using the *Gaia* DR3 photometry (G magnitude and

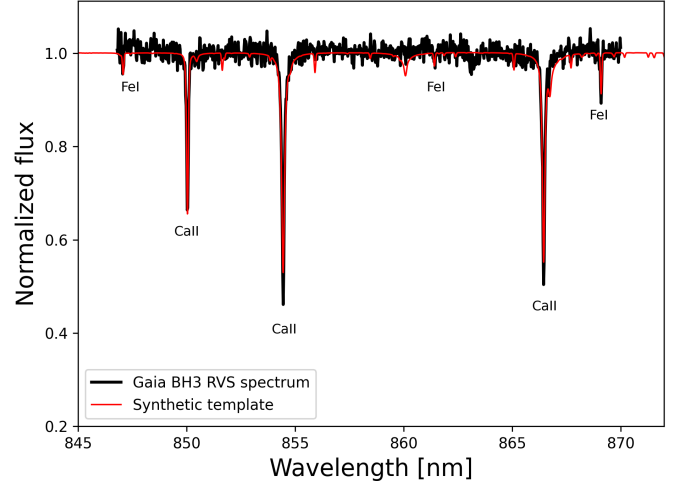


Fig. 4. *Gaia* RVS combined spectrum of *Gaia* BH3, in restframe, compared with the template spectrum.

Table 3. Stellar parameters of *Gaia* BH3 derived in this work.

Parameter	Value
T_{eff} [K]	5212 ± 80
$\log g$	2.929 ± 0.003
[Fe/H]	-2.56 ± 0.11
[α /Fe]	0.43 ± 0.12
[M/H]	-2.21 ± 0.15
$\log(L_{\star}/L_{\odot})$	1.208 ± 0.030
M_{\star} [M_{\odot}]	0.76 ± 0.05
R_{\star} [R_{\odot}]	4.936 ± 0.016
$M_{G,0}$ [mag]	1.778 ± 0.082
$(G_{\text{BP}} - G_{\text{RP}})_0$ [mag]	0.921 ± 0.031

$G_{\text{BP}} - G_{\text{RP}}$ colour), the parallax from the combined astrometric-spectroscopic solution, and the extinction (A_0) derived from the dust extinction maps of Vergely et al. (2022), with an iterative procedure described in Appendix D. The UVES spectrum was used to determine the metallicity and abundances (see Appendix E). We then compared the extinction-corrected absolute G magnitude ($M_{G,0}$) and the dereddened colour $(G_{\text{BP}} - G_{\text{RP}})_0$ with the ones given by the isochrones libraries PARSEC (Bressan et al. 2012) and BaSTI (Pietrinfermi et al. 2021). Thus, we derived the mass (M_{\star}) of the visible component. The parameters are reported in Table 3.

In Fig. 5, we compare the expected spectral energy distribution (SED) with the *Gaia* XP spectrum (Carrasco et al. 2021; De Angeli et al. 2023; Montegriffo et al. 2023) and 2MASS photometry. The agreement between the predicted SED and the *Gaia* XP spectrum is very good, with the only exception of the blue edge, where the XP spectrum is noisier.

The abundances of *Gaia* BH3 (reported in Appendix E) show that the star is α -enhanced, as expected for a very metal-poor star. There is no trace of ^{13}C in the spectrum and the [Ba/Fe] is nearly solar, indicating the star has not been enriched by material processed in the CNO cycle, as expected if it had, for instance, accreted material from a companion star in the AGB phase. The star has no chemical peculiarity, except an enhancement of Eu ([Eu/Fe] = 0.52). Thus, it can be classified as an r-I neutron-capture-rich star, following the classification of Beers & Christlieb (2005).

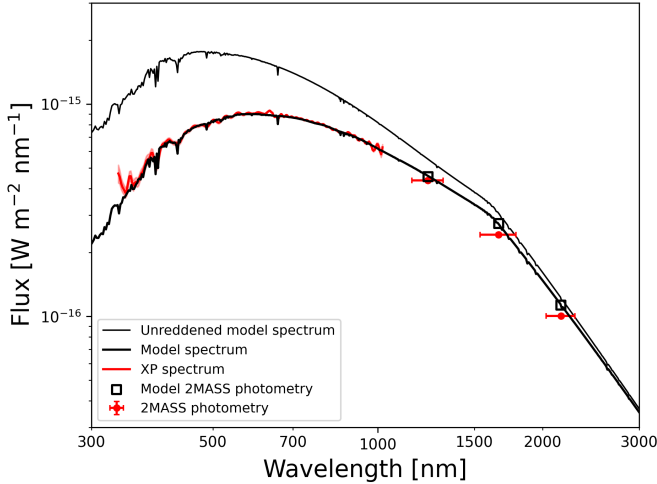


Fig. 5. *Gaia* BH3 modelled SED, compared with the *Gaia* XP spectrum and 2MASS photometry. The thin black line shows the unreddened model, while the thick line shows the SED assuming $A_0 = 0.71$ mag.

Using the systemic radial velocity, proper motion, position, and distance, and assuming the Milky Way gravitational potential from McMillan (2017), we may find that the source has a high-energy retrograde orbit³ ($E = -1.29 \times 10^5 \text{ km}^2 \text{ s}^{-2}$, $L_z = -2.3 \times 10^3 \text{ kpc km s}^{-1}$, $L_\perp = 1.05 \times 10^3 \text{ kpc km s}^{-1}$) in the Galaxy. Its kinematic characteristics are consistent with those of the halo substructure known as Sequoia (Myeong et al. 2019), but are also in agreement to those of the recently discovered ED-2 stream (Dodd et al. 2023; Balbinot et al. 2023), a likely remnant of a globular cluster that was disrupted by the Milky Way. The metallicity of *Gaia* BH3 is more consistent with ED-2 ($[\text{Fe}/\text{H}] = -2.6 \pm 0.2$) than with the median metallicity of Sequoia ($[\text{Fe}/\text{H}] \sim -1.7$).

3. Discussion

With an estimated mass of $0.76 \pm 0.05 M_\odot$ for the luminous companion, we derived a mass of:

$$M_{\text{BH}} = 32.70 \pm 0.82 M_\odot, \quad (5)$$

for the dark companion. The observed luminosity of *Gaia* BH3 is too low by several orders of magnitude to be compatible with the hypothesis that the companion is a main sequence star or even two main sequence stars in a close orbit. The estimated mass is also too large for one neutron star or two neutron stars in a close orbit, so we are left with the possibility of: (1) a single BH; (2) an inner binary containing two BHs; or (3) a BH and another compact object. Although the single BH is the simplest explanation, the hypothesis of an inner binary of two BHs cannot be excluded. Hayashi et al. (2023) proposed a method to test this hypothesis by detecting radial-velocity perturbations at the periastron. Using the Hayashi et al. (2023) formulation, we estimated radial-velocity perturbations⁴ with a maximum amplitude of the order of 0.2 km s^{-1} . Such perturbations are too small to be detected in the *Gaia* RVS data, but can be verified with ground-based instruments (see Nagarajan et al. 2024, for an application

³ Here we use the same conventions as in Myeong et al. (2019).

⁴ We use $K_{\text{short}}(1 - e)^{-7/2}$ as perturbations level estimation, (see Sect. 2.1 in Hayashi et al. 2023), assuming an inner equal-mass binary with a circular coplanar orbit, and a period corresponding to the maximum allowed by dynamic stability (126 days, according to Eq. (6) in Hayashi et al. 2023).

to *Gaia* BH1). For the purposes of the subsequent discussion, we have adopted the single BH hypothesis as the most likely explanation.

The estimated mass of the BH in *Gaia* BH3 makes it the most massive BH of stellar origin discovered in our Galaxy. It is striking that the only BH with a mass larger than $20 M_\odot$ found in the *Gaia* data so far is in orbit with a very metal-poor star, while such stars make up only a tiny fraction of the stars analysed in the NSS pipeline run (0.4% of sources which produced a binary solution have $[\text{M}/\text{H}] < -2$ from DR3 GSP-Phot). Such stars also make up a small fraction of our Galactic halo (less than 5% according to Bonifacio et al. 2021) where this star and the majority of metal-poor stars are located. Although we can not exclude that this BH is the result of the merger of two less massive BHs, this discovery strongly supports the scenario where high-mass BHs are remnants of low-metallicity stars. The above considerations also raise the question of the maximum metallicity value for the formation of high-mass BHs, which in Belczynski et al. (2016) is identified at $[\text{M}/\text{H}] = -1$. The much lower metallicity of *Gaia* BH3 may be an indication that high-mass BHs form only at very low metallicities rather than at moderately low ones.

An in-depth discussion of the possible formation scenarios for this binary system is beyond the scope of the paper; nevertheless, a few aspects ought to be highlighted. As discussed in El-Badry et al. (2023b,a), the formation of the *Gaia* BH1 and BH2 systems as isolated binaries is unlikely. This is also true for the recently discovered *Gaia* NS1 system (El-Badry et al. 2024), composed of a high-mass neutron star and a low-metallicity star. Given the size of their orbits, these systems should have experienced a common-envelope phase and then a mass transfer toward the light companion, which would then have resulted in much closer orbits than the observed ones. For *Gaia* BH2, the common-envelope phase could have been avoided if the BH progenitor was more massive than $65 M_\odot$. In the case of *Gaia* BH3, the present-day minimum separation is of the order of $1000 R_\odot$ and the common-envelope phase could not have been avoided because models predict that the BH progenitor becomes a red supergiant even at $150 M_\odot$ (Chen et al. 2015). Similarly to *Gaia* BH1 and BH2, the chemical composition of the luminous component does not show any unusual abundance; in particular, the absence of ^{13}C and the observed $[\text{Ba}/\text{Fe}]$ point toward a lack of contamination by the BH progenitor during its evolution. The observed enhanced Eu abundance could be due to the contamination from the SN at the birth of the BH, but also due to the medium in which the star formed. An alternative formation scenario, proposed to explain the *Gaia* BH1 and BH2 systems, is that the BH acquired the low-mass companion via dynamical exchange in a dense environment (see for example Rastello et al. 2023; Tanikawa et al. 2024; Di Carlo et al. 2024). Such a scenario might be supported by the probable association of *Gaia* BH3 with the ED-2 stream, which could be a remnant of a globular cluster (Dodd et al. 2023; Balbinot et al. 2023).

4. Conclusions

In this Letter, we present the discovery of a wide binary composed of a very metal-poor giant orbiting a dark object of $33 M_\odot$, using *Gaia* preliminary DR4 astrometric data, corroborated by *Gaia* spectroscopy. Most probably, the massive dark object is a single black hole (BH). The $33 M_\odot$ of the BH mass makes it the most massive BH of stellar origin discovered in our Galaxy. All Galactic BHs that reside in short-period X-ray binaries have masses generally below $10 M_\odot$ (e.g. Corral-Santana et al. 2016), except Cyg-X1 ($M_{\text{BH}} \sim 20 M_\odot$). Even the first two dormant BHs

discovered by *Gaia* in wide astrometric orbits have masses of about $10 M_{\odot}$. The mass of *Gaia* BH3 puts it in the mass range of the BHs discovered by gravitational waves (e.g. Abbott et al. 2023), and, in fact, it is close to the peak of the observed mass distribution for the merging BHs (e.g. Farah et al. 2024). The metallicity of the system supports the scenario (Belczynski et al. 2016) that the high-mass BHs observed by LIGO/Virgo/KAGRA (Abbott et al. 2020a) are the remnants of metal-poor stars.

The discovered system, with its extremely low-mass ratio, wide orbit, and specific chemical composition, can also provide constraints for stellar evolution and binary models. As in the case of the *Gaia* BH1 and BH2 systems, the formation scenario as an isolated binary appears unlikely and alternative scenarios should be considered. The BHs discovered by *Gaia* in wide binaries in our Galaxy and those detected by LIGO/Virgo/KAGRA in external galaxies (i.e. BH merger events of extremely short-period binaries) constitute two ends of the BH population. When studied together, they can help to formulate a comprehensive view of BH formation and the evolution of their progenitors.

Finally, the bright magnitude of the system and its relatively small distance makes it an easy target for further observations and detailed analyses by the astronomical community. This discovery should be also seen as a preliminary teaser for the content of *Gaia* DR4, which will undoubtedly reveal other binary systems hosting a BH.

Acknowledgements. This work has made use of data from the European Space Agency (ESA) mission *Gaia* (<https://www.cosmos.esa.int/gaia>), processed by the *Gaia* Data Processing and Analysis Consortium (DPAC, <https://www.cosmos.esa.int/web/gaia/dpac/consortium>). Funding for the DPAC has been provided by national institutions, in particular the institutions participating in the *Gaia* Multilateral Agreement. Based on observations made with the *Mercator* Telescope, operated on the island of La Palma by the Flemish Community, at the Spanish Observatorio del Roque de los Muchachos of the Instituto de Astrofísica de Canarias. Based on observations obtained with the HERMES spectrograph, which is supported by the Research Foundation – Flanders (FWO), Belgium, the Research Council of KU Leuven, Belgium, the Fonds National de la Recherche Scientifique (F.R.S.-FNRS), Belgium, the Royal Observatory of Belgium, the Observatoire de Genève, Switzerland and the Thüringer Landessternwarte Tautenburg, Germany. This publication has also made use of observations collected with the SOPHIE spectrograph on the 1.93-m telescope at Observatoire de Haute-Provence (CNRS), France (program 23B.PNPS.AREN) using support by the French Programme National de Physique Stellaire (PNPS). Based on observations collected at the European Southern Observatory under ESO programme 106.211J.001. We warmly thank Piercarlo Bonifacio for help with the use of ATLAS9 models and helpful discussions, Hans Van Winckel, HERMES PI, for granting observational time, and Rosine Lallement for helpful discussions on the use of extinction maps. We thank the referee for comments that helped to improve the paper. The full acknowledgements are available in Appendix F.

References

Abbott, B. P., Abbott, R., Abbott, T. D., et al. 2016, *Phys. Rev. Lett.*, **116**, 061102
 Abbott, B. P., Abbott, R., Abbott, T. D., et al. 2020a, *Liv. Rev. Relativ.*, **23**, 3
 Abbott, R., Abbott, T. D., Abraham, S., et al. 2020b, *ApJ*, **900**, L13
 Abbott, R., Abbott, T. D., Abraham, S., et al. 2021, *ApJ*, **913**, L7
 Abbott, R., Abbott, T. D., Acernese, F., et al. 2023, *Phys. Rev. X*, **13**, 011048
 Ahn, C. P., Alexandroff, R., Allende Prieto, C., et al. 2012, *ApJS*, **203**, 21
 Albaret, F. D., Allende Prieto, C., Almeida, A., et al. 2017, *ApJS*, **233**, 25
 Andrae, R., Fouesneau, M., Sordo, R., et al. 2023, *A&A*, **674**, A27
 Astropy Collaboration (Price-Whelan, A. M., et al.) 2018, *AJ*, **156**, 123
 Babusiaux, C., Fabricius, C., Khanna, S., et al. 2023, *A&A*, **674**, A32
 Balbinot, E., Helmi, A., Callingham, T., et al. 2023, *A&A*, **678**, A115
 Bavera, S. S., Fragos, T., Zapartas, E., et al. 2023, *Nat. Astron.*, **7**, 1090
 Beers, T. C., & Christlieb, N. 2005, *ARA&A*, **43**, 531
 Belczynski, K., Taam, R. E., Kalogera, V., Rasio, F. A., & Bulik, T. 2007, *ApJ*, **662**, 504
 Belczynski, K., Bulik, T., Fryer, C. L., et al. 2010a, *ApJ*, **714**, 1217
 Belczynski, K., Dominik, M., Bulik, T., et al. 2010b, *ApJ*, **715**, L138

Belczynski, K., Holz, D. E., Bulik, T., & O’Shaughnessy, R. 2016, *Nature*, **534**, 512
 Bergemann, M., Lind, K., Collet, R., Magic, Z., & Asplund, M. 2012, *MNRAS*, **427**, 27
 Bergemann, M., Collet, R., Amarsi, A. M., et al. 2017, *ApJ*, **847**, 15
 Blomme, R., Edvardsson, B., Eriksson, K., et al. 2021, *Synthetic spectra used by CU6 in DR2*, Gaia Data Processing and Analysis Consortium (DPAC) Technical Note GAIA-C6-TN-ROB-RHB-005, <http://www.cosmos.esa.int/web/gaia/public-dpac-documents>
 Boch, T., & Fernique, P. 2014, *ASP Conf. Ser.*, **485**, 277
 Bonifacio, P., Monaco, L., Salvadori, S., et al. 2021, *A&A*, **651**, A79
 Bonnarel, F., Fernique, P., Bienaymé, O., et al. 2000, *A&AS*, **143**, 33
 Bovy, J. 2015, *ApJS*, **216**, 29
 Breddels, M. A., & Veljanoski, J. 2018, *A&A*, **618**, A13
 Bressan, A., Marigo, P., Girardi, L., et al. 2012, *MNRAS*, **427**, 127
 Caffau, E., Ludwig, H. G., Steffen, M., Freytag, B., & Bonifacio, P. 2011, *Sol. Phys.*, **268**, 255
 Carrasco, J. M., Weiler, M., Jordi, C., et al. 2021, *A&A*, **652**, A86
 Casagrande, L., & Vandenberg, D. A. 2014, *MNRAS*, **444**, 392
 Castelli, F., & Kurucz, R. L. 2003, in *Modelling of Stellar Atmospheres*, eds. N. Piskunov, W. W. Weiss, & D. F. Gray, 210, A20
 Chakrabarti, S., Simon, J. D., Craig, P. A., et al. 2023, *AJ*, **166**, 6
 Chambers, K. C., Magnier, E. A., Metcalfe, N., et al. 2016, ArXiv e-prints [arXiv:1612.05560]
 Chen, Y., Bressan, A., Girardi, L., et al. 2015, *MNRAS*, **452**, 1068
 Corral-Santana, J. M., Casares, J., Muñoz-Darias, T., et al. 2016, *A&A*, **587**, A61
 Creevey, O. L., Sordo, R., Pailler, F., et al. 2023, *A&A*, **674**, A26
 Cropper, M., Katz, D., Sartoretti, P., et al. 2018, *A&A*, **616**, A5
 De Angeli, F., Weiler, M., Montegriffo, P., et al. 2023, *A&A*, **674**, A2
 Dekker, H., D’Odorico, S., Kaufer, A., Delabre, B., & Kotzlowski, H. 2000, *SPIE Conf. Ser.*, **4008**, 534
 Di Carlo, U. N., Agrawal, P., Rodriguez, C. L., & Breivik, K. 2024, *ApJ*, **965**, 22
 Dodd, E., Callingham, T. M., Helmi, A., et al. 2023, *A&A*, **670**, L2
 El-Badry, K., Rix, H.-W., Cendes, Y., et al. 2023a, *MNRAS*, **521**, 4323
 El-Badry, K., Rix, H.-W., Quataert, E., et al. 2023b, *MNRAS*, **518**, 1057
 El-Badry, K., Simon, J. D., Reggiani, H., et al. 2024, *Open J. Astrophys.*, **7**, 27
 Fabricius, C., Høg, E., Makarov, V. V., et al. 2002, *A&A*, **384**, 180
 Fabricius, C., Bastian, U., Portell, J., et al. 2016, *A&A*, **595**, A3
 Farah, A. M., Fishbach, M., & Holz, D. E. 2024, *ApJ*, **962**, 69
 Fitzpatrick, E. L., Massa, D., Gordon, K. D., Bohlin, R., & Clayton, G. C. 2019, *ApJ*, **886**, 108
 Flewelling, H. A., Magnier, E. A., Chambers, K. C., et al. 2020, *ApJS*, **251**, 7
 Fouesneau, M., Frémat, Y., Andrae, R., et al. 2023, *A&A*, **674**, A28
 Frebel, A., Casey, A. R., Jacobson, H. R., & Yu, Q. 2013, *ApJ*, **769**, 57
 Fryer, C. L., Belczynski, K., Wiktorowicz, G., et al. 2012, *ApJ*, **749**, 91
 Gaia Collaboration (Prusti, T., et al.) 2016, *A&A*, **595**, A1
 Gaia Collaboration (Arenou, F., et al.) 2023a, *A&A*, **674**, A34
 Gaia Collaboration (Vallenari, A., et al.) 2023b, *A&A*, **674**, A1
 Giesers, B., Dreizler, S., Husser, T. -O., et al. 2018, *MNRAS*, **475**, L15
 Gilmore, G., Randich, S., Worley, C. C., et al. 2022, *A&A*, **666**, A120
 Górski, K. M., Hivon, E., Banday, A. J., et al. 2005, *ApJ*, **622**, 759
 Gosset, E., Damerjji, Y., Morel, T., et al. 2024, *A&A*, submitted
 Halbwachs, J. L. 2009, *MNRAS*, **394**, 1075
 Halbwachs, J.-L., Pourbaix, D., Arenou, F., et al. 2023, *A&A*, **674**, A9
 Hayashi, T., Suto, Y., & Trani, A. A. 2023, *ApJ*, **958**, 26
 Henden, A. A., Templeton, M., Terrell, D., et al. 2016, *VizieR Online Data Catalogue: II/336*
 Høg, E., Fabricius, C., Makarov, V. V., et al. 2000, *A&A*, **355**, L27
 Holl, B., Fabricius, C., Portell, J., et al. 2023, *A&A*, **674**, A25
 Huber, D., Bryson, S. T., Haas, M. R., et al. 2016, *ApJS*, **224**, 2
 Hunter, J. D. 2007, *Comput. Sci. Eng.*, **9**, 90
 Hurley, J. R., Pols, O. R., & Tout, C. A. 2000, *MNRAS*, **315**, 543
 Katz, D., Sartoretti, P., Guerrier, A., et al. 2023, *A&A*, **674**, A5
 Korotin, S. A., Andrievsky, S. M., Hansen, C. J., et al. 2015, *A&A*, **581**, A70
 Kovalev, M., Brinkmann, S., Bergemann, M., & MPA IT-department 2018, *NLTE MPA Web Server* (Heidelberg: Max Planck Institute for Astronomy), <http://nlte.mpia.de>
 Kurucz, R. L. 2005, *Mem. Soc. Astron. It. Suppl.*, **8**, 14
 Lallement, R., Vergely, J. L., Babusiaux, C., & Cox, N. L. J. 2022, *A&A*, **661**, A147
 Lam, C. Y., Lu, J. R., Udalski, A., et al. 2022, *ApJ*, **933**, L23
 Lasker, B. M., Lattanzi, M. G., McLean, B. J., et al. 2008, *AJ*, **136**, 735
 Lépine, S., & Shara, M. M. 2005, *AJ*, **129**, 1483
 Lindegren, L., & Bastian, U. 2022, *Local plane coordinates for the detailed analysis of complex Gaia sources*, Gaia Data Processing and Analysis Consortium (DPAC) technical note GAIA-C3-TN-LU-LL-061, <http://www.cosmos.esa.int/web/gaia/public-dpac-documents>
 Lindegren, L., Lammers, U., Hobbs, D., et al. 2012, *A&A*, **538**, A78

- Lindegren, L., Bastian, U., Biermann, M., et al. 2021a, *A&A*, 649, A4
- Lindegren, L., Klioner, S. A., Hernández, J., et al. 2021b, *A&A*, 649, A2
- Lodders, K., Palme, H., & Gail, H. P. 2009, *Landolt Börnstein*, 4B, 712
- Lombardo, L., François, P., Bonifacio, P., et al. 2021, *A&A*, 656, A155
- Luo, A. L., Zhao, Y. H., Zhao, G., et al. 2015, *Res. Astron. Astrophys.*, 15, 1095
- Magnier, E. A., Chambers, K. C., Flewelling, H. A., et al. 2020a, *ApJS*, 251, 3
- Magnier, E. A., Schlafly, E. F., Finkbeiner, D. P., et al. 2020b, *ApJS*, 251, 6
- Magnier, E. A., Sweeney, W. E., Chambers, K. C., et al. 2020c, *ApJS*, 251, 5
- Mapelli, M., Colpi, M., & Zampieri, L. 2009, *MNRAS*, 395, L71
- Mashonkina, L., Korn, A. J., & Przybilla, N. 2007, *A&A*, 461, 261
- McMillan, P. J. 2017, *MNRAS*, 465, 76
- Miller-Jones, J. C. A., Bahramian, A., Orosz, J. A., et al. 2021, *Science*, 371, 1046
- Montegriffo, P., De Angeli, F., Andrae, R., et al. 2023, *A&A*, 674, A3
- Mucciarelli, A., Salaris, M., & Bonifacio, P. 2012, *MNRAS*, 419, 2195
- Myeong, G. C., Vasiliev, E., Iorio, G., Evans, N. W., & Belokurov, V. 2019, *MNRAS*, 488, 1235
- Nagarajan, P., El-Badry, K., Triaud, A. H. M. J., et al. 2024, *PASP*, 136, 014202
- Ochsenbein, F., Bauer, P., & Marcout, J. 2000, *A&AS*, 143, 23
- Olejak, A., Belczynski, K., Bulik, T., & Sobolewska, M. 2020, *A&A*, 638, A94
- Onken, C. A., Wolf, C., Bessell, M. S., et al. 2019, *PASA*, 36, e033
- Pérez, F., & Granger, B. E. 2007, *Comput. Sci. Eng.*, 9, 21
- Perruchot, S., Kohler, D., Bouchy, F., et al. 2008, *SPIE Conf. Ser.*, 7014, 70140J
- Pietrinferni, A., Hidalgo, S., Cassisi, S., et al. 2021, *ApJ*, 908, 102
- Pourbaix, D., Arenou, F., Gavras, P., et al. 2022, *Gaia DR3 documentation Chapter 7: Non-Single Stars*, <https://gea.esac.esa.int/archive/documentation/GDR3/index.html>, 7
- Randich, S., Gilmore, G., Magrini, L., et al. 2022, *A&A*, 666, A121
- Raskin, G., van Winckel, H., Hensberge, H., et al. 2011, *A&A*, 526, A69
- Rastello, S., Iorio, G., Mapelli, M., et al. 2023, *MNRAS*, 526, 740
- R Core Team 2013, *R: A Language and Environment for Statistical Computing* (Vienna, Austria: R Foundation for Statistical Computing)
- Recio-Blanco, A., de Laverny, P., Palicio, P. A., et al. 2023, *A&A*, 674, A29
- Riello, M., De Angeli, F., Evans, D. W., et al. 2021, *A&A*, 649, A3
- Roeser, S., Demleitner, M., & Schilbach, E. 2010, *AJ*, 139, 2440
- Sahlmann, J. 2019, <https://doi.org/10.5281/zenodo.3315526>
- Sahu, K. C., Anderson, J., Casertano, S., et al. 2022, *ApJ*, 933, 83
- Salaris, M., Chieffi, A., & Straniero, O. 1993, *ApJ*, 414, 580
- Saracino, S., Kamann, S., Guarcello, M. G., et al. 2022, *MNRAS*, 511, 2914
- Sartoretti, P., Blomme, R., David, M., & Seabroke, G. 2022, *Gaia DR3 documentation Chapter 6: Spectroscopy*, <https://gea.esac.esa.int/archive/documentation/GDR3/index.html>, 6
- Sartoretti, P., Katz, D., Cropper, M., et al. 2018, *A&A*, 616, A6
- Sartoretti, P., Marchal, O., Babusiaux, C., et al. 2023, *A&A*, 674, A6
- Sbordone, L., Caffau, E., Bonifacio, P., & Duffau, S. 2014, *A&A*, 564, A109
- Sitnova, T. M., Yakovleva, S. A., Belyaev, A. K., & Mashonkina, L. I. 2022, *MNRAS*, 515, 1510
- Skrutskie, M. F., Cutri, R. M., Stiening, R., et al. 2006, *AJ*, 131, 1163
- Steinmetz, M., Guiglion, G., McMillan, P. J., et al. 2020a, *AJ*, 160, 83
- Steinmetz, M., Matijević, G., Enke, H., et al. 2020b, *AJ*, 160, 82
- Sukhbold, T., Ertl, T., Woosley, S. E., Brown, J. M., & Janka, H. T. 2016, *ApJ*, 821, 38
- Tanikawa, A., Hattori, K., Kawanaka, N., et al. 2023, *ApJ*, 946, 79
- Tanikawa, A., Cary, S., Shikauchi, M., Wang, L., & Fujii, M. S. 2024, *MNRAS*, 527, 4031
- Tantalo, R., Chiosi, C., & Bressan, A. 1998, *A&A*, 333, 419
- Taylor, M. B. 2005, *ASP Conf. Ser.*, 347, 29
- Taylor, M. B. 2006, *ASP Conf. Ser.*, 351, 666
- Ulla, A., Creevey, O. L., Álvarez, M. A., et al. 2022, *Gaia DR3 documentation Chapter 11: Astrophysical parameters*, <https://gea.esac.esa.int/archive/documentation/GDR3/index.html>, 11
- van Leeuwen, F. 2007, *A&A*, 474, 653
- Vergely, J. L., Lallement, R., & Cox, N. L. J. 2022, *A&A*, 664, A174
- Vink, J. S. 2008, *New Astron. Rev.*, 52, 419
- Waters, C. Z., Magnier, E. A., Price, P. A., et al. 2020, *ApJS*, 251, 4
- Wenger, M., Ochsenbein, F., Egret, D., et al. 2000, *A&AS*, 143, 9
- Zacharias, N., Finch, C. T., Girard, T. M., et al. 2013, *AJ*, 145, 44
- Zacharias, N., Finch, C., Subasavage, J., et al. 2015, *AJ*, 150, 101
- Ziosi, B. M., Mapelli, M., Branchesi, M., & Tormen, G. 2014, *MNRAS*, 441, 3703
- ³ Department of Astronomy, University of Geneva, Chemin Pegasi 51, 1290 Versoix, Switzerland
- ⁴ Department of Astronomy, University of Geneva, Chemin d'Ecogia 16, 1290 Versoix, Switzerland
- ⁵ Institut d'Astronomie et d'Astrophysique, Université Libre de Bruxelles CP 226, Boulevard du Triomphe, 1050 Brussels, Belgium
- ⁶ Univ. Grenoble Alpes, CNRS, IPAG, 38000 Grenoble, France
- ⁷ RHEA for European Space Agency (ESA), Camino bajo del Castillo, s/n, Urbanización Villafranca del Castillo, Villanueva de la Cañada 28692, Madrid, Spain
- ⁸ Astronomisches Rechen-Institut, Zentrum für Astronomie der Universität Heidelberg, Mönchhofstr. 12-14, 69120 Heidelberg, Germany
- ⁹ Astronomical Observatory, University of Warsaw, Al. Ujazdowskie 4, 00-478 Warszawa, Poland
- ¹⁰ HE Space Operations BV for European Space Agency (ESA), Camino bajo del Castillo, s/n, Urbanización Villafranca del Castillo, Villanueva de la Cañada 28692, Madrid, Spain
- ¹¹ Mullard Space Science Laboratory, University College London, Holmbury St Mary, Dorking, Surrey RH5 6NT, UK
- ¹² Telespazio UK S.L. for European Space Agency (ESA), Camino bajo del Castillo, s/n, Urbanización Villafranca del Castillo, Villanueva de la Cañada, 28692 Madrid, Spain
- ¹³ Kapteyn Astronomical Institute, University of Groningen, Landleven 12, 9747 AD Groningen, The Netherlands
- ¹⁴ Leiden Observatory, Leiden University, Einsteinweg 55, 2333 CC Leiden, The Netherlands
- ¹⁵ INAF – Osservatorio astronomico di Padova, Vicolo Osservatorio 5, 35122 Padova, Italy
- ¹⁶ European Space Agency (ESA), European Space Research and Technology Centre (ESTEC), Keplerlaan 1, 2201 AZ Noordwijk, The Netherlands
- ¹⁷ CNES Centre Spatial de Toulouse, 18 avenue Edouard Belin, 31401 Toulouse Cedex 9, France
- ¹⁸ Université Côte d'Azur, Observatoire de la Côte d'Azur, CNRS, Laboratoire Lagrange, Bd de l'Observatoire, CS 34229, 06304 Nice Cedex 4, France
- ¹⁹ Laboratoire d'astrophysique de Bordeaux, Univ. Bordeaux, CNRS, B18N, allée Geoffroy Saint-Hilaire, 33615 Pessac, France
- ²⁰ Institute of Astronomy, University of Cambridge, Madingley Road, Cambridge CB3 0HA, UK
- ²¹ European Space Agency (ESA), European Space Astronomy Centre (ESAC), Camino bajo del Castillo, s/n, Urbanización Villafranca del Castillo, Villanueva de la Cañada 28692, Madrid, Spain
- ²² Aurora Technology for European Space Agency (ESA), Camino bajo del Castillo, s/n, Urbanización Villafranca del Castillo, Villanueva de la Cañada 28692, Madrid, Spain
- ²³ Institut de Ciències del Cosmos (ICCUB), Universitat de Barcelona (UB), Martí i Franquès 1, 08028 Barcelona, Spain
- ²⁴ Institut d'Estudis Espacials de Catalunya (IEEC), c. Esteve Terradas 1, 08860 Castelldefels, (Barcelona), Spain
- ²⁵ Lohrmann Observatory, Technische Universität Dresden, Mommsenstraße 13, 01062 Dresden, Germany
- ²⁶ Lund Observatory, Division of Astrophysics, Department of Physics, Lund University, Box 43, 22100 Lund, Sweden
- ²⁷ Departament de Física Quàntica i Astrofísica (FQA), Universitat de Barcelona (UB), c. Martí i Franquès 1, 08028 Barcelona, Spain
- ²⁸ INAF – Osservatorio Astrofisico di Arcetri, Largo Enrico Fermi 5, 50125 Firenze, Italy
- ²⁹ Nicolaus Copernicus Astronomical Center, Polish Academy of Sciences, ul. Bartycka 18, 00-716 Warsaw, Poland
- ³⁰ Instituut voor Sterrenkunde, KU Leuven, Celestijnenlaan 200D, 3001 Leuven, Belgium
- ³¹ Department of Astrophysics/IMAPP, Radboud University, PO Box 9010, 6500 GL Nijmegen, The Netherlands
- ³² Max Planck Institute for Astronomy, Königstuhl 17, 69117 Heidelberg, Germany
- ³³ INAF – Osservatorio Astrofisico di Torino, Via Osservatorio 20, 10025 Pino Torinese, (TO), Italy

¹ GEPI, Observatoire de Paris, Université PSL, CNRS, 5 Place Jules Janssen, 92190 Meudon, France

e-mail: pasquale.panuzzo@observatoiredeparis.psl.eu

² School of Physics and Astronomy, Tel Aviv University, Tel Aviv 6997801, Israel

- ³⁴ European Space Agency (ESA, retired), European Space Research and Technology Centre (ESTEC), Keplerlaan 1, 2201 AZ Noordwijk, The Netherlands
- ³⁵ University of Turin, Department of Physics, Via Pietro Giuria 1, 10125 Torino, Italy
- ³⁶ Royal Observatory of Belgium, Ringlaan 3, 1180 Brussels, Belgium
- ³⁷ DAPCOM Data Services, c. dels Vilabella, 5-7, 80500 Vic, Barcelona, Spain
- ³⁸ Observational Astrophysics, Division of Astronomy and Space Physics, Department of Physics and Astronomy, Uppsala University, Box 516, 751 20 Uppsala, Sweden
- ³⁹ ALTEC S.p.a, Corso Marche, 79, 10146 Torino, Italy
- ⁴⁰ Sednai Sàrl, Geneva, Switzerland
- ⁴¹ Gaia DPAC Project Office, ESAC, Camino bajo del Castillo, s/n, Urbanización Villafranca del Castillo, Villanueva de la Cañada 28692, Madrid, Spain
- ⁴² SYRTE, Observatoire de Paris, Université PSL, CNRS, Sorbonne Université, LNE, 61 avenue de l'Observatoire, 75014 Paris, France
- ⁴³ IMCCE, Observatoire de Paris, Université PSL, CNRS, Sorbonne Université, Univ. Lille, 77 av. Denfert-Rochereau, 75014 Paris, France
- ⁴⁴ INAF – Osservatorio di Astrofisica e Scienza dello Spazio di Bologna, Via Piero Gobetti 93/3, 40129 Bologna, Italy
- ⁴⁵ Serco Gestión de Negocios for European Space Agency (ESA), Camino bajo del Castillo, s/n, Urbanización Villafranca del Castillo, Villanueva de la Cañada 28692, Madrid, Spain
- ⁴⁶ Institut d'Astrophysique et de Géophysique, Université de Liège, 19c, Allée du 6 Août, 4000 Liège, Belgium
- ⁴⁷ CRAAG – Centre de Recherche en Astronomie, Astrophysique et Géophysique, Route de l'Observatoire Bp 63, Bouzareah 16340, Algiers, Algeria
- ⁴⁸ Institute for Astronomy, University of Edinburgh, Royal Observatory, Blackford Hill, Edinburgh EH9 3HJ, UK
- ⁴⁹ CIGUS CITIC – Department of Computer Science and Information Technologies, University of A Coruña, Campus de Elviña s/n, A Coruña 15071, Spain
- ⁵⁰ Kavli Institute for Cosmology Cambridge, Institute of Astronomy, Madingley Road, Cambridge CB3 0HA, UK
- ⁵¹ Department of Astrophysics, Astronomy and Mechanics, National and Kapodistrian University of Athens, Panepistimiopolis, Zografos 15783, Athens, Greece
- ⁵² Donald Bren School of Information and Computer Sciences, University of California, Irvine, CA 92697, USA
- ⁵³ CENTRA, Faculdade de Ciências, Universidade de Lisboa, Edif. C8, Campo Grande, 1749-016 Lisboa, Portugal
- ⁵⁴ INAF – Osservatorio Astrofisico di Catania, Via S. Sofia 78, 95123 Catania, Italy
- ⁵⁵ Dipartimento di Fisica e Astronomia “Ettore Majorana”, Università di Catania, Via S. Sofia 64, 95123 Catania, Italy
- ⁵⁶ Université de Strasbourg, CNRS, Observatoire astronomique de Strasbourg, UMR 7550, 11 rue de l'Université, 67000 Strasbourg, France
- ⁵⁷ INAF – Osservatorio Astronomico di Roma, Via Frascati 33, 00078 Monte Porzio Catone, (Roma), Italy
- ⁵⁸ Space Science Data Center – ASI, Via del Politecnico SNC, 00133 Roma, Italy
- ⁵⁹ Department of Physics, University of Helsinki, PO Box 64, 00014 Helsinki, Finland
- ⁶⁰ Finnish Geospatial Research Institute FGI, Vuorimiehentie 5, 02150 Espoo, Finland
- ⁶¹ Institut UTINAM CNRS UMR6213, Université de Franche-Comté, OSU THETA Franche-Comté Bourgogne, Observatoire de Besançon, BP1615, 25010 Besançon Cedex, France
- ⁶² HE Space Operations BV for European Space Agency (ESA), Keplerlaan 1, 2201 AZ Noordwijk, The Netherlands
- ⁶³ Dpto. de Inteligencia Artificial, UNED, c/ Juan del Rosal 16, 28040 Madrid, Spain
- ⁶⁴ Leibniz Institute for Astrophysics Potsdam (AIP), An der Sternwarte 16, 14482 Potsdam, Germany
- ⁶⁵ Konkoly Observatory, HUN-REN Research Centre for Astronomy and Earth Sciences, MTA Centre of Excellence, 1121 Konkoly Thege Miklós út 15-17, Budapest, Hungary
- ⁶⁶ Institute of Physics and Astronomy, ELTE Eötvös Loránd University, 1117 Pázmány Péter sétány 1A, Budapest, Hungary
- ⁶⁷ University of Vienna, Department of Astrophysics, Türkenschanzstraße 17, A1180 Vienna, Austria
- ⁶⁸ ATG Europe for European Space Agency (ESA), Camino bajo del Castillo, s/n, Urbanización Villafranca del Castillo, Villanueva de la Cañada 28692 Madrid, Spain
- ⁶⁹ Institute of Physics, Ecole Polytechnique Fédérale de Lausanne (EPFL), Observatoire de Sauvigny, 1290 Versoix, Switzerland
- ⁷⁰ Centre for Astrophysics Research, University of Hertfordshire, College Lane AL10 9AB, Hatfield, UK
- ⁷¹ Quasar Science Resources for European Space Agency (ESA), Camino bajo del Castillo, s/n, Urbanización Villafranca del Castillo, Villanueva de la Cañada 28692, Madrid, Spain
- ⁷² LASIGE, Faculdade de Ciências, Universidade de Lisboa, Edif. C6, Campo Grande 1749-016, Lisboa, Portugal
- ⁷³ School of Physics and Astronomy, University of Leicester, University Road, Leicester LE1 7RH, UK
- ⁷⁴ Astrophysics Group, Cavendish Laboratory, University of Cambridge, JJ Thomson Avenue, Cambridge CB3 0HE, UK
- ⁷⁵ Thales Services for CNES Centre Spatial de Toulouse, 18 avenue Edouard Belin, 31401 Toulouse Cedex 9, France
- ⁷⁶ Telespazio for CNES Centre Spatial de Toulouse, 18 avenue Edouard Belin, 31401 Toulouse Cedex 9, France
- ⁷⁷ National Observatory of Athens, I. Metaxa and Vas. Pavlou, Palaia Penteli 15236, Athens, Greece
- ⁷⁸ University of Maryland, College Park, MD, USA
- ⁷⁹ EURIX S.r.l., Corso Vittorio Emanuele II 61, 10128 Torino, Italy
- ⁸⁰ Porter School of the Environment and Earth Sciences, Tel Aviv University, Tel Aviv 6997801, Israel
- ⁸¹ Harvard-Smithsonian Center for Astrophysics, 60 Garden St., MS 15, Cambridge, MA 02138, USA
- ⁸² Laboratoire de Recherche en Neuroimagerie, University Hospital (CHUV) and University of Lausanne (UNIL), Lausanne, Switzerland
- ⁸³ Sydney Institute for Astronomy, School of Physics, University of Sydney, Sydney, NSW 2006, Australia
- ⁸⁴ ARC Centre of Excellence for All Sky Astrophysics in 3 Dimensions (ASTRO 3D), Mt. Stromlo, Australia
- ⁸⁵ ATOS for CNES Centre Spatial de Toulouse, 18 avenue Edouard Belin, 31401 Toulouse Cedex 9, France
- ⁸⁶ Department of Physics and Astronomy G. Galilei, University of Padova, Vicolo dell'Osservatorio 3, 35122 Padova, Italy
- ⁸⁷ LFCA/DAS, Universidad de Chile, CNRS, Casilla 36-D, Santiago, Chile
- ⁸⁸ University of West Attica, Ag. Spyridonos Str., Egaleo 12243, Athens, Greece
- ⁸⁹ SISSA – Scuola Internazionale Superiore di Studi Avanzati, via Bonomea 265, 34136 Trieste, Italy
- ⁹⁰ SII for CNES Centre Spatial de Toulouse, 18 avenue Edouard Belin, 31401 Toulouse Cedex 9, France
- ⁹¹ University of Turin, Department of Computer Sciences, Corso Svizzera 185, 10149 Torino, Italy
- ⁹² Dpto. de Matemática Aplicada y Ciencias de la Computación, Univ. de Cantabria, ETS Ingenieros de Caminos, Canales y Puertos, Avda. de los Castros s/n, 39005 Santander, Spain
- ⁹³ Institut de Física d'Altes Energies (IFAE), The Barcelona Institute of Science and Technology, Campus UAB, 08193 Bellaterra, (Barcelona), Spain
- ⁹⁴ Port d'Informació Científica (PIC), Campus UAB, C. Albareda s/n, 08193 Bellaterra, (Barcelona), Spain
- ⁹⁵ Centro de Investigaciones Energéticas, Medioambientales y Tecnológicas (CIEMAT), Avenida Complutense 40, 28040 Madrid, Spain
- ⁹⁶ Monash University, 10 College Walk, Monash University, Clayton, VIC 3800, Australia

- ⁹⁷ Ruder Bošković Institute, Bijenička cesta 54, 10000 Zagreb, Croatia
- ⁹⁸ Universidad Andres Bello, Facultad de Ciencias Exactas, Departamento de Ciencias Físicas – Instituto de Astrofísica, Fernandez Concha 700, Las Condes, Santiago, Chile
- ⁹⁹ LESIA, Observatoire de Paris, Université PSL, CNRS, Sorbonne Université, Université de Paris, 5 Place Jules Janssen, 92190 Meudon, France
- ¹⁰⁰ University of Turin, Mathematical Department “G.Peano”, Via Carlo Alberto 10, 10123 Torino, Italy
- ¹⁰¹ University of Antwerp, Onderzoeksgroep Toegepaste Wiskunde, Middelheimlaan 1, 2020 Antwerp, Belgium
- ¹⁰² INAF – Osservatorio Astronomico d’Abruzzo, Via Mentore Maggini, 64100 Teramo, Italy
- ¹⁰³ APAVE EXPLOITATION for CNES Centre Spatial de Toulouse, 18 avenue Edouard Belin, 31401 Toulouse Cedex 9, France
- ¹⁰⁴ Dpto. Física Teórica y del Cosmos, Universidad de Granada, 18071 Granada, Spain
- ¹⁰⁵ The Center for Cosmology and Particle Physics, New York University, 726 Broadway, New York, NY 10003, USA
- ¹⁰⁶ Finnish Centre for Astronomy with ESO, University of Turku, 20014 Turku, Finland
- ¹⁰⁷ Astrophysics Research Centre, School of Mathematics and Physics, Queen’s University Belfast, Belfast BT7 1NN, UK
- ¹⁰⁸ Institute for Computational Cosmology, Department of Physics, Durham University, Durham DH1 3LE, UK
- ¹⁰⁹ Data Science and Big Data Lab, Pablo de Olavide University, 41013 Seville, Spain
- ¹¹⁰ Institute of Astrophysics, FORTH, Crete, Greece
- ¹¹¹ Barcelona Supercomputing Center (BSC), Plaça Eusebi Güell 1-3, 08034 Barcelona, Spain
- ¹¹² Center for Astrophysics and Cosmology, University of Nova Gorica, Vipavska 13, 5000 Nova Gorica, Slovenia
- ¹¹³ F.R.S.-FNRS, Rue d’Egmont 5, 1000 Brussels, Belgium
- ¹¹⁴ Asteroid Engineering Laboratory, Luleå University of Technology, Box 848, 981 28 Kiruna, Sweden
- ¹¹⁵ IAC – Instituto de Astrofísica de Canarias, Via Láctea s/n, 38200 La Laguna S.C., Tenerife, Spain
- ¹¹⁶ Department of Astrophysics, University of La Laguna, Via Láctea s/n, 38200 La Laguna S.C., Tenerife, Spain
- ¹¹⁷ Las Cumbres Observatory, 6740 Cortona Drive Suite 102, Goleta, CA 93117, USA
- ¹¹⁸ Université Rennes, CNRS, IPR (Institut de Physique de Rennes), UMR 6251, 35000 Rennes, France
- ¹¹⁹ INAF – Osservatorio Astronomico di Capodimonte, Via Moiariello 16, 80131 Napoli, Italy
- ¹²⁰ Shanghai Astronomical Observatory, Chinese Academy of Sciences, 80 Nandan Road, Shanghai 200030, PR China
- ¹²¹ University of Chinese Academy of Sciences, No.19(A) Yuquan Road, Shijingshan District, Beijing 100049, PR China
- ¹²² São Paulo State University, Grupo de Dinâmica Orbital e Planetologia, CEP 12516-410, Guaratinguetá, SP, Brazil
- ¹²³ CIGUS CITIC, Department of Nautical Sciences and Marine Engineering, University of A Coruña, Paseo de Ronda 51, 15071 A Coruña, Spain
- ¹²⁴ Astrophysics Research Institute, Liverpool John Moores University, 146 Brownlow Hill, Liverpool L3 5RF, UK
- ¹²⁵ IRAP, Université de Toulouse, CNRS, UPS, CNES, 9 Av. colonel Roche, BP 44346, 31028 Toulouse Cedex 4, France
- ¹²⁶ Serco Gestión de Negocios for European Space Agency (ESA), Camino bajo del Castillo, s/n, Urbanización Villafranca del Castillo, Villanueva de la Cañada 28692 Madrid, Spain
- ¹²⁷ Astronomical Institute, Faculty of Mathematics and Physics, Charles University, V Holešovičkách 2, 180 00 Prague, Czech Republic
- ¹²⁸ Dribia Data Research S.L., Pg. de Gràcia 55, 3r 4a, 08007, Barcelona, Spain
- ¹²⁹ Pioneer Research Center for Climate and Earth Science, Institute for Basic Science, Daejeon 34126, Republic of Korea
- ¹³⁰ Astronomical Observatory, Jagiellonian University, ul. Orła 171, 30-244 Kraków, Poland
- ¹³¹ Center for Computational Astrophysics, Flatiron Institute, 162 Fifth Ave, New York, NY 10010, USA
- ¹³² INAF – Osservatorio Astronomico di Brera, Via E. Bianchi, 46, 23807 Merate, (LC), Italy
- ¹³³ National Astronomical Observatory of Japan, 2-21-1 Osawa, Mitaka, Tokyo 181-8588, Japan
- ¹³⁴ Department of Particle Physics and Astrophysics, Weizmann Institute of Science, Rehovot 7610001, Israel
- ¹³⁵ Centre de Données Astronomiques de Strasbourg, Strasbourg, France
- ¹³⁶ Astrophysics Group, Department of Physics and Astronomy, University of Exeter, Exeter EX4 4QL, UK
- ¹³⁷ Departamento de Astrofísica, Centro de Astrobiología (CSIC-INTA), ESA-ESAC, Camino Bajo del Castillo s/n, 28692 Villanueva de la Cañada, Madrid, Spain
- ¹³⁸ naXys, Department of Mathematics, University of Namur, Rue de Bruxelles 61, 5000 Namur, Belgium
- ¹³⁹ INAF. Osservatorio Astronomico di Trieste, Via G.B. Tiepolo 11, 34131 Trieste, Italy
- ¹⁴⁰ H H Wills Physics Laboratory, University of Bristol, Tyndall Avenue, Bristol BS8 1TL, UK
- ¹⁴¹ Instituto de Astronomia, Geofísica e Ciências Atmosféricas, Universidade de São Paulo, Rua do Matão, 1226, Cidade Universitária, 05508-900 São Paulo, SP, Brazil
- ¹⁴² Escuela de Arquitectura y Politécnica – Universidad Europea de Valencia, Valencia, Spain
- ¹⁴³ Escuela Superior de Ingeniería y Tecnología – Universidad Internacional de la Rioja, Rioja, Spain
- ¹⁴⁴ Institut für Physik und Astronomie, Universität Potsdam, Haus 28, Karl-Liebknecht-Str. 24/25, 14476 Golm, (Potsdam), Germany
- ¹⁴⁵ Applied Physics Department, Universidade de Vigo, 36310 Vigo, Spain
- ¹⁴⁶ Instituto de Física e Ciências Aeroespaciais (IFCAE), Universidade de Vigo Campus de As Lagoas, 32004 Ourense, Spain
- ¹⁴⁷ Purple Mountain Observatory and Key Laboratory of Radio Astronomy, Chinese Academy of Sciences, 10 Yuanhua Road, Nanjing 210033, PR China
- ¹⁴⁸ Sorbonne Université, CNRS, UMR7095, Institut d’Astrophysique de Paris, 98bis bd. Arago, 75014 Paris, France
- ¹⁴⁹ Faculty of Mathematics and Physics, University of Ljubljana, Jadranska ulica 19, 1000 Ljubljana, Slovenia

Appendix A: Astrometric processing in the NSS 4.1 run

Here, we provide the details of the Non-Single Star (NSS) pipeline used in the preliminary run NSS 4.1, underlining this is not the final version of the NSS pipeline for the generation of *Gaia* DR4 data.

The pipeline is similar to the one used in *Gaia* DR3 (Halbwachs et al. 2023), with a few updates – the main differences are in the improvement of the filters to remove spurious solutions. In particular, two new filters were introduced to remove sources which are partially resolved: the first one filters out sources with significant scan-angle-dependent signals (Holl et al. 2023) in the G flux before attempting an astrometric solution; the second one removes solutions which have periods that correspond to combinations of the *Gaia* spacecraft precession frequency and the yearly frequency (see Holl et al. 2023, Sect. 4.1). These new filters allow us to relax the filters based on the significance and on ϖ/σ_ϖ , described in Halbwachs et al. (2023), which are replaced by the following criteria: the goodness-of-fit (GoF) must be smaller than 15, the eccentricity error smaller than 0.2, semi-major axis significance $a_0/\sigma_{a_0} > 5$, and

$$\varpi/\sigma_\varpi > \max(15, -208.02 \cdot \log(P/1 \text{ day}) + 548.03). \quad (\text{A.1})$$

The NSS 4.1 run was executed using astrometric data produced with preliminary runs (namely IDU 4.1 and AGIS 4.1) of the Intermediate Data Update (IDU; see Fabricius et al. 2016) and the Astrometric Global Iterative Solution (AGIS; see Lindegren et al. 2021b) pipelines. The preliminary astrometry provided by AGIS 4.1 covers the entire range of DR4, i.e. from JD 2456863.9385 to JD 2458869.4177, for a total of about 67 months, but only data after JD 2456941.6218 were used in the NSS 4.1 run. The local perspective effect (Halbwachs 2009) was not included in the model for the run NSS 4.1 and the variability-induced mover (VIM) solutions were not attempted.

The NSS 4.1 run was executed on a list of 10 450 939 sources chosen with the following criteria: the source must be brighter than $G_{\text{RVS}} = 14$ mag and either $G < 18$ mag, an astrometric renormalised unit weight error (RUWE) larger than 1.05, or $\varpi > 5$ mas and $\text{RUWE} > 0.9$, and a number of visibility periods used in AGIS solution larger than 11. In order to exclude partially resolved sources, sources with a percent of successful Image Parameter Determination (IPD) windows with more than one peak larger than 10% or with amplitudes of the IPD GoF versus the scan angle larger than 0.2, were excluded (see *Gaia* DR3 archive documentation for details on the above quantities). The run produced a total of 1 469 196 orbital solutions.

The selection function of the NSS 4.1 run is not trivial to characterise, thus, it is not possible to estimate how common or rare are systems like *Gaia* BH3. If we push *Gaia* BH3 to the distance corresponding to the cut in magnitude ($G_{\text{RVS}} = 14$ mag would correspond to a distance of 3.3 kpc, ignoring the extinction), the semi-major axis of the orbit would be 4.8 mas, which is still very large with respect to the precision of *Gaia* epoch measurements at that magnitude. However, given that the DR4 time range covers only half of the orbital period, the resulting significance could be below the acceptance thresholds. We note that during the *Gaia* DR3 preparation, *Gaia* BH3 produced an astrometric acceleration solution (Halbwachs et al. 2023) and an SB1 solution (Gosset et al. 2024), which were both discarded from the release due to a low significance, because the orbital period was much longer than the *Gaia* DR3 time span and the periastron passage was not covered by the DR3 time range.

If we consider a *Gaia* BH3-like system but with an orbital period similar or shorter of the DR4 time range (i.e. below 2000 days), the significance would be always higher than the acceptance threshold solution, with the exception of very short (<20 day) periods. We note that the NSS 4.1 is limited to periods larger than 10 days. For binaries with shorter periods, the giant would almost fill its Roche lobe and the source would probably be detected as a X-ray source.

Although it has not yet been finalised, the input list for DR4 will be significantly larger than for NSS 4.1, probably built as the sum of a volume-limited sample and a $G < 18$ magnitude-limited sample, as indicated above, though without the $G_{\text{RVS}} < 14$ mag criterion. The motivation for the dedicated NSS 4.1 run and the reason for the latter criterion was the analysis of the effect of a deviation of the astrometry from the assumed single-star model on the calibration of the spectroscopic instrument.

Appendix B: *Gaia* epoch data

Here, we describe the *Gaia* epoch astrometric data and epoch radial velocities used to produce the binary solution of *Gaia* BH3.

The astrometric measurements of *Gaia* BH3 are provided in Table B.1. They were produced from preliminary pipelines, provisional instrument models and calibrations; as a consequence they will not be identical (but still similar) to the corresponding data to be produced and published for this star with DR4. Furthermore, the final epoch astrometry table in DR4 will contain many additional details and quality diagnostics on the individual measurements. A full explanation of the epoch astrometry is beyond the scope of the present short appendix. We refer the reader to the *Gaia* Technical Document Lindegren & Bastian (2022) and to Lindegren et al. (2012).

Each *Gaia* epoch astrometry record in Table B.1 corresponds to a transit of the source on one of the CCDs of the AF instrument. The Table is arranged as follows. Col. 1: `transit_id`⁵, a unique identifier assigned to each detected celestial light source as its image transits the *Gaia* focal plane; Col. 2: AF CCD strip; Col. 3: Barycentric time, in JD, corresponding to the middle of the 4.41-second CCD exposure time; Col. 4: Along-scan position of the photocentre, with its associated uncertainty, which corresponds to the longitude of the observed photocentre in a 2D tangential coordinate system having its origin at a reference equatorial position, and having the axis of its longitude coordinate oriented corresponding to the scanning direction; Col. 5: Parallax factor, namely, the quantity by which it is necessary to multiply the parallax in order to obtain the contribution to the along-scan position due to the orbit of the spacecraft with respect to the Solar System barycentre; Col. 6: Scan angle, which is the angle of the scanning direction with respect to local ICRS North; Col. 7: Outlier flag, indicating whether the measurement was considered as an outlier (flag = 1) by the NSS pipeline and filtered out, or not (flag = 0), when solving for the astrometric-spectroscopic combined solution.

The reference position (α_0, δ_0), in the sense of Lindegren & Bastian (2022), for *Gaia* BH3 is

$$\alpha_0 = 294^\circ 82784900557243, \delta_0 = 14^\circ 930918410309376, \quad (\text{B.1})$$

while the reference time is J2017.5 (JD 2457936.875).

⁵ A decoder for the `transit_id` is available on-line at <https://gaia.esac.esa.int/decoder/transitidDecoder.jsp>

Table B.1. *Gaia* BH3 epoch astrometry.

transit_id	AF strip	Time [BJD, TCB]	Along-scan position [mas]	Parallax factor	Scan angle [deg]	Outlier flag
20114916805338633	1	2456958.110978	147.066 ± 0.370	0.70827985	-59.04672662	0
20114916805338633	2	2456958.111034	146.696 ± 0.231	0.70827991	-59.04677105	0
20114916805338633	3	2456958.111091	146.685 ± 0.183	0.70828003	-59.04681553	0
20114916805338633	4	2456958.111156	146.557 ± 0.151	0.70828015	-59.04686711	0
20114916805338633	5	2456958.111203	146.396 ± 0.097	0.70828021	-59.04690435	0
20114916805338633	6	2456958.111259	146.374 ± 0.088	0.70828027	-59.04694869	0
20114916805338633	7	2456958.111325	146.436 ± 0.100	0.70828038	-59.04700014	0
20114916805338633	8	2456958.111372	146.060 ± 0.100	0.70828044	-59.04703723	1
20114916805338633	9	2456958.111437	146.256 ± 0.130	0.70828056	-59.04708855	0
20119009095238725	1	2456958.184993	146.244 ± 0.364	0.70847327	-59.11055165	0
20119009095238725	2	2456958.185043	146.148 ± 0.296	0.70847344	-59.11059886	0
20119009095238725	3	2456958.185105	146.192 ± 0.267	0.70847368	-59.11065699	0
20119009095238725	4	2456958.185162	146.271 ± 0.225	0.70847386	-59.11070963	0
20119009095238725	5	2456958.185218	146.047 ± 0.273	0.70847410	-59.11076223	0
20119009095238725	6	2456958.185274	146.068 ± 0.158	0.70847428	-59.11081482	0
20119009095238725	7	2456958.185330	146.023 ± 0.177	0.70847452	-59.11086742	0
20119009095238725	8	2456958.185386	146.095 ± 0.191	0.70847470	-59.11092003	0
...

Notes. The full table is available at the CDS.

Table B.2. *Gaia* BH3 epoch radial velocities from *Gaia* RVS.

transit_id	Time [BJD, TCB]	Radial velocity [km s ⁻¹]
22989619581449144	2457010.096166	-338.62 ± 1.42
22993711812243969	2457010.170169	-341.08 ± 1.70
27565894819405940	2457092.856649	-338.73 ± 1.41
27569987068420645	2457092.930660	-340.63 ± 1.43
29624665178404300	2457130.091203	-335.28 ± 2.20
37997278005744779	2457281.508798	-330.88 ± 1.24
52687653750370648	2457547.177378	-320.11 ± 1.61
60072325242450363	2457680.722202	-319.09 ± 1.87
61702852954182073	2457710.207118	-315.11 ± 1.12
68202800816349412	2457827.754668	-305.82 ± 1.53
81052816639971536	2458060.142534	-290.29 ± 1.42
82486181452083612	2458086.062277	-294.93 ± 1.53
82490273693622584	2458086.136278	-294.67 ± 1.75
100312802889225719	2458408.450948	-404.70 ± 1.14
111669627072959442	2458613.834346	-399.65 ± 1.21
112765863248582085	2458633.660613	-398.97 ± 1.10
121996985218154856	2458800.596176	-393.59 ± 2.00

Notes. The table is also available at the CDS.

Epoch RVS radial velocities, reported in Table B.2, were produced with the final pipeline, but not finalised with the post-processing; their values or uncertainties may slightly differ from the final DR4 values. As for the astrometry, the final epoch radial velocity table in DR4 will contain additional details and quality diagnostics on the individual measurements. Each epoch radial velocity record in Table B.2 corresponds to a transit of the source on the RVS CCDs. The provided observation time of the radial velocity corresponds to the mean of the observation times of the three CCDs used to collect spectra in the RVS during the transit.

A public code, illustrating the use of epoch astrometric and radial velocity data to produce an orbital solution for *Gaia* BH3 is available online⁶.

Appendix C: Ground-based spectroscopy

Table C.1. *Gaia* BH3 epoch radial velocities from ground-based observations.

Instrument	Time [BJD, UTC]	Radial velocity [km s ⁻¹]
UVES	2459158.5333	-383.20 ± 0.30
HERMES	2460143.4948	-364.05 ± 0.20
SOPHIE	2460192.4359	-363.15 ± 0.02
HERMES	2460193.4833	-363.24 ± 0.20

We observed *Gaia* BH3 with the HERMES spectrograph (Raskin et al. 2011) mounted on the 1.2-meter *Mercator* telescope at the Roque de los Muchachos Observatory (Spain), at two dates (17 July 2023 and 7 September 2023), taking two consecutive exposures of 2700 s each night. The spectra have a spectral coverage from 377 to 900 nm, a resolving power of 85 000, and a S/N ~ 43 at 520 nm.

We observed *Gaia* BH3 also with the SOPHIE spectrograph (Perruchot et al. 2008) mounted on the 1.93-meter telescope of the Observatoire de Haute-Provence (France) on 4 September 2023. The source was observed with a single exposure of 6000 s; the spectra cover the range 387 to 694 nm with a resolving power of 40 000, and have a S/N ~ 66 at 520 nm. HERMES and SOPHIE spectra of *Gaia* BH3 are available on request from the corresponding author.

A search in the ESO archive revealed that the source was observed with the UVES spectrograph (Dekker et al. 2000)

⁶ <https://www.cosmos.esa.int/web/gaia/gaia-bhthree>

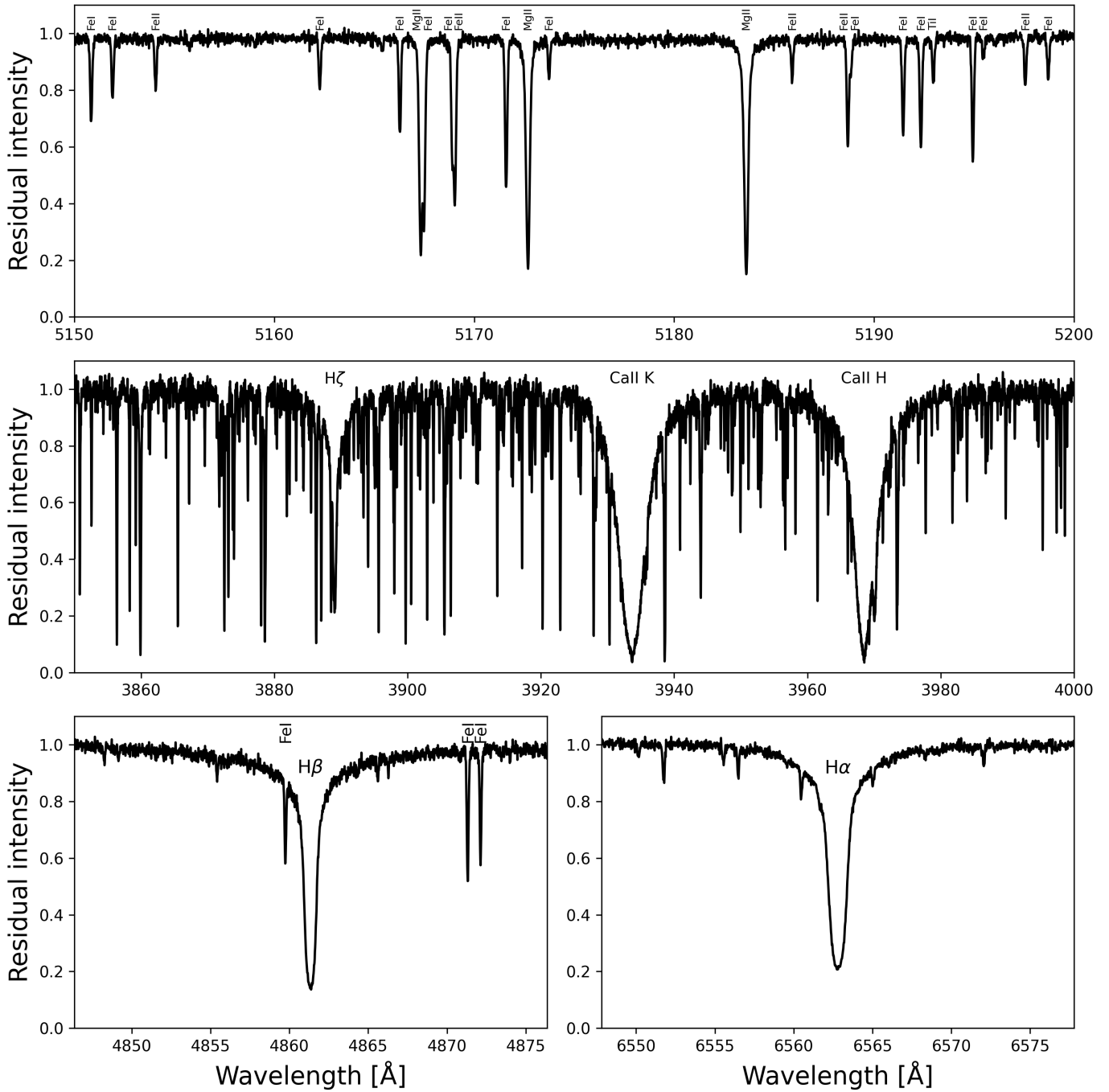


Fig. C.1. Residual intensity of the *Gaia* BH3 UVES spectrum in the magnesium triplet region (top panel), in the Ca II H+K region (middle panel), H β (bottom-left) and H α (bottom-right).

mounted on the VLT, on 5 November 2020, in the program 106.21JJ.001 proposed by T. Matsuno and collaborators. The aim of the program was to derive a complete chemical inventory of stars belonging to Galactic accretion events. The exposure time of the UVES spectrum was 900 s in the 390+580 setting (spectral coverage 326 to 454 nm and 476 to 684 nm) with a slit of 0.7'', producing a resolving power of 58 000 in the blue and 62 000 in the red and a S/N \sim 100 at 520 nm.

For HERMES and SOPHIE observations, radial velocities were derived by computing the cross-correlation functions with a G2 mask, while for the UVES spectrum the radial velocity was derived via template matching. The barycentric radial-

velocity values are reported in Table C.1, and they are in good agreement with the orbit derived from *Gaia* data. The spectra do not show any sign of the presence of a second component, nor any emission line. The UVES normalised spectrum of the *Gaia* BH3 in selected spectral regions is shown in Fig. C.1.

Appendix D: Derivation of stellar parameters

Here we describe the iterative procedure used to derive the stellar parameters of the luminous component in *Gaia* BH3. The procedure is similar to the one adopted in Lombardo et al. (2021).

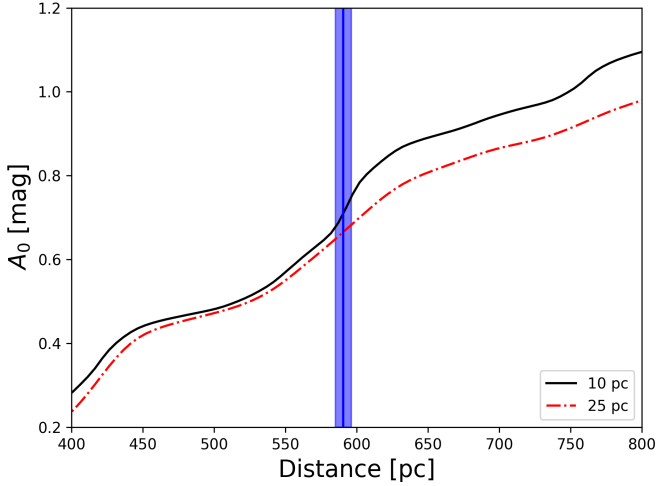


Fig. D.1. Extinction in the direction of *Gaia* BH3, as function of the distance. The extinction was derived with the maps with correlation length of 10 pc (black solid line) and 25 pc (red dot-dashed line) from Vergely et al. (2022); the vertical shaded region shows the distance range of *Gaia* BH3.

We computed the emerging flux for a grid in T_{eff} , $\log g$ and $[\text{Fe}/\text{H}]$, of 1D plane-parallel model atmospheres, using ATLAS 9 (Castelli et al. 2003; Kurucz 2005). The fluxes were then converted to spectral energy distributions by multiplying them by a factor $4\pi(R_{\odot}/10\text{pc})^2$, where R_{\odot} is the solar radius, as done in Casagrande & Vandenberg (2014). All models were computed assuming $[\alpha/\text{Fe}] = 0.4$. For each model, we computed theoretical values of the color $G_{\text{BP}} - G_{\text{RP}}$, the bolometric correction (BC_G), and the extinction coefficients A_G/A_0 and $E(G_{\text{BP}} - G_{\text{RP}})/A_0$, using the average Milky Way reddening law from Fitzpatrick et al. (2019).

The iterative procedure starts with first-guess metallicity, temperature and gravity from *Gaia* DR3 values reported in Table 1, a first-guess mass (M_{\star}) of $0.8 M_{\odot}$, and a given reddening of A_0 . We use the above parameters to obtain $E(G_{\text{BP}} - G_{\text{RP}})$ from the grid, which is then used to obtain a dereddened $G_{\text{BP}} - G_{\text{RP}}$ colour, $(G_{\text{BP}} - G_{\text{RP}})_0$, the extinction A_G , and the bolometric correction BC_G . We then compare the $(G_{\text{BP}} - G_{\text{RP}})_0$ value to theoretical colours in the grid to derive a new effective temperature, and we use the Stefan-Boltzmann equation to derive a new surface gravity:

$$\log g = \log \frac{M_{\star}}{M_{\odot}} + 4 \log \frac{T_{\text{eff}}}{T_{\odot}} + \log g_{\odot} + 0.4(G - A_G + \text{BC}_G - m_{\text{bol},\odot}) + 2 \log \frac{\varpi}{1000 \text{ mas}}. \quad (\text{D.1})$$

The procedure is repeated to convergence in T_{eff} and $\log g$ which is achieved after a few iterations. The parameters T_{eff} and $\log g$ are then used to derive the metallicity $[\text{Fe}/\text{H}]$ as described in Sect. E and the process repeated.

The T_{eff} , $\log g$, and $[\text{Fe}/\text{H}]$ derived with the above procedure depend mainly on the choice of A_0 . *Gaia* BH3 has a low Galactic latitude ($b = -3.49^{\circ}$), located in a zone with a relatively high gradient of A_0 , according to extinction maps of Vergely et al. (2022), as can be seen in Fig. D.1. Adopting a distance of 590.6 ± 5.8 pc, we obtain $A_0 = 0.710^{+0.041}_{-0.034}$ mag for a correlation length of 10 pc and $A_0 = 0.666 \pm 0.017$ mag for a correlation length of 25 pc. We thus adopted $A_0 = 0.71 \pm 0.07$ mag.

An updated value for M_{\star} can be then estimated by comparing the absolute G magnitude, $M_{G,0}$ and the colour $(G_{\text{BP}} - G_{\text{RP}})_0$

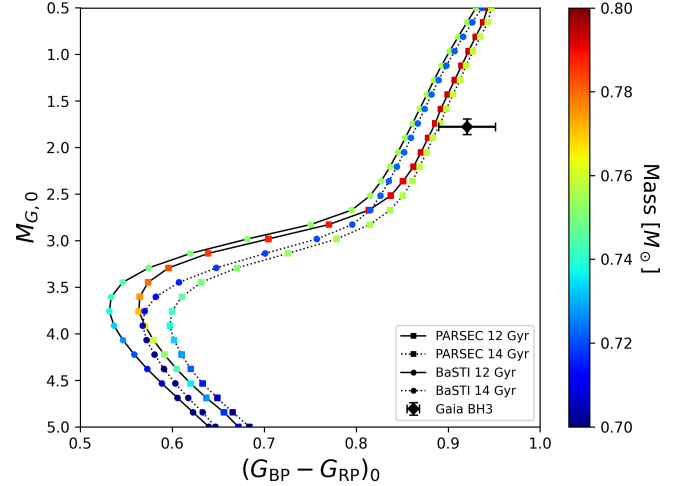


Fig. D.2. Comparison between the position of *Gaia* BH3 and isochrones in the colour-magnitude diagram. The colours of the symbols (filled circles for BaSTI and filled squares for PARSEC), on the two isochrones sets (12 and 14 Gyr), correspond to the stellar masses.

with the ones given by theoretical isochrones. The procedure for the determination of stellar parameters is finally repeated with the updated value of M_{\star} .

The value of M_{\star} depends mainly on the assumed age and isochrone set, while it has a very small dependency on the assumed A_0 . We used isochrones from both PARSEC⁷ (Bressan et al. 2012) and BaSTI⁸ (Pietrinferni et al. 2021) libraries. For BaSTI, we adopt $[\text{Fe}/\text{H}] = -2.5$, $[\alpha/\text{Fe}] = 0.4$ and $[\text{M}/\text{H}] = -2.18$, while for PARSEC isochrones, which are only available with no α -enhancement, we use metallicity $[\text{Fe}/\text{H}] = -2.18$, i.e. we scale the $[\text{Fe}/\text{H}]$ to match the $[\text{M}/\text{H}]$ of BaSTI isochrones and take into account the contribution of α -elements to the total metallicity (e.g. Salaris et al. 1993). The comparison between isochrones and *Gaia* BH3 in the $M_{G,0}$ versus $(G_{\text{BP}} - G_{\text{RP}})_0$ diagram is shown in Fig. D.2.

The value of M_{\star} goes from 0.758 to $0.793 M_{\odot}$ for PARSEC and 0.723 to $0.755 M_{\odot}$ for BaSTI, for isochrone of ages 12 and 14 Gyr, respectively. Younger ages would result in higher masses, but also bluer colours. We then estimate a mass $M_{\star} = 0.76 \pm 0.05 M_{\odot}$ as the mass for the visible companion.

With the procedure described above, we obtain the following parameters: $T_{\text{eff}} = 5211 \pm 80$ K, $\log g = 2.929 \pm 0.003$, $[\text{Fe}/\text{H}] = -2.56 \pm 0.12$. From the Mg I and Ca I abundances, we derived an α -enhancement of $[\alpha/\text{Fe}] = 0.43 \pm 0.12$. Using the relation between iron content, enhancement and metallicity from Tantaló et al. (1998), we obtain $[\text{M}/\text{H}] = -2.21 \pm 0.15$.

It can be seen that the source is slightly redder and cooler than what is predicted by the models, albeit not significantly. In order to check that the T_{eff} that we determined above is not underestimated, we derived an alternative temperature estimation from the excitation equilibrium of the Fe I lines, including the NLTE corrections by Frebel et al. (2013). With this method, we obtained $T_{\text{eff}} \sim 5100$ K, which is even cooler, confirming that our estimation is not underestimated. A more detailed analysis of the stellar parameters is outside the scope of this work.

⁷ <http://stev.oapd.inaf.it/cgi-bin/cmd>

⁸ <http://basti-iac.iaa-brunswick.inaf.it/isocs.html>

Table E.1. Abundances of *Gaia* BH3 from UVES spectrum.

Ion	N_{lines}	A(X)	[X/H]	$\sigma_{A(X)}$		NLTE corr.
				(1)	(2)	
C I	...	6.11	-2.39	0.10	0.17	...
Mg I	5	5.46	-2.08	0.05	0.04	0.06 ^a
Ca I	20	4.13	-2.20	0.10	0.05	0.14 ^b
Sc II	6	0.76	-2.34	0.11	0.03	...
Ti I	17	2.67	-2.23	0.06	0.11	...
Ti II	26	2.80	-2.10	0.08	0.04	...
V I	3	1.34	-2.66	0.13	0.10	...
V II	6	1.61	-2.39	0.07	0.03	...
Cr I	5	2.86	-2.78	0.01	0.08	...
Cr II	3	3.23	-2.41	0.06	0.03	...
Mn I	7	2.45	-2.92	0.04	0.04	...
Mn II	1	2.79	-2.58	...	0.08	...
Fe I	223	4.96	-2.56	0.12	0.08	0.10 ^c
Fe II	15	5.03	-2.49	0.13	0.01	...
Co I	7	2.62	-2.30	0.09	0.11	...
Ni I	18	3.68	-2.55	0.12	0.06	...
Zn I	1	2.22	-2.40	...	0.02	0.12 ^d
Sr II	2	0.50	-2.42	0.05	0.08	...
Y II	10	-0.44	-2.65	0.16	0.05	...
Zr II	6	0.34	-2.28	0.12	0.05	...
Ba II	4	-0.28	-2.45	0.13	0.06	-0.10 ^e
La II	4	-1.22	-2.36	0.07	0.05	...
Eu II	1	-1.45	-1.97	...	0.05	...

Notes. The values A(X) are expressed in the form $A(X) = \log(X/H) + 12$, while $[X/H] = \log(A(X)/A(X)_{\odot})$. The uncertainties on the abundances ($\sigma_{A(X)}$) are reported as (1) line-to-line dispersion or (2) effect of T_{eff} uncertainty. NLTE corrections are from ^aBergemann et al. (2017) ^bMashonkina et al. (2007) ^cBergemann et al. (2012) ^dSitnova et al. (2022) ^eKorotin et al. (2015)

Appendix E: Abundances

We estimated the metallicity and abundances of the luminous component of *Gaia* BH3 from the UVES spectrum, which is of higher quality than our HERMES and SOPHIE spectra.

The abundances were derived with the code **MYGIESFOS** (Sbordone et al. 2014), with the exception of those for C, Ba and Eu; the carbon abundance was derived by fitting the Fraunhofer *G*-band of the CH molecule, while line-profile fitting was used to determine Ba and Eu abundances. The resulting values are listed in Table E.1. In the table, we provide the line-to-line scatter and the variation of the abundance corresponding to the uncertainty on the effective temperature. We adopted the solar abundances for C, Fe and Eu from Caffau et al. (2011), and those from Lodders et al. (2009) for the other elements. We derived a value of 1.19 km s^{-1} for the micro-turbulence, by forcing the same Fe abundance from Fe I lines of different equivalent width.

We sought the non-local thermal equilibrium (NLTE) correction for Mg I and Ca I in Kovalev et al. (2018). For the four Mg I lines available, we derived a NLTE correction of 0.06. Eleven lines of Ca I provided a NLTE correction of 0.15. The five Cr I lines available in the database provide a large NLTE correction: 0.46. For the Mn I features, the NLTE correction is 0.54. The 67 Fe I lines available provide a mean NLTE correction of 0.1. The NLTE effect on the Zn I line at 481 nm in Sitnova et al. (2022) and the Ba in Korotin et al. (2015) are small (see Table E.1).

The [Fe/H] ratio we derived from the UVES spectrum ([Fe/H] = -2.56 ± 0.12 from 223 Fe I lines) is in perfect agree-

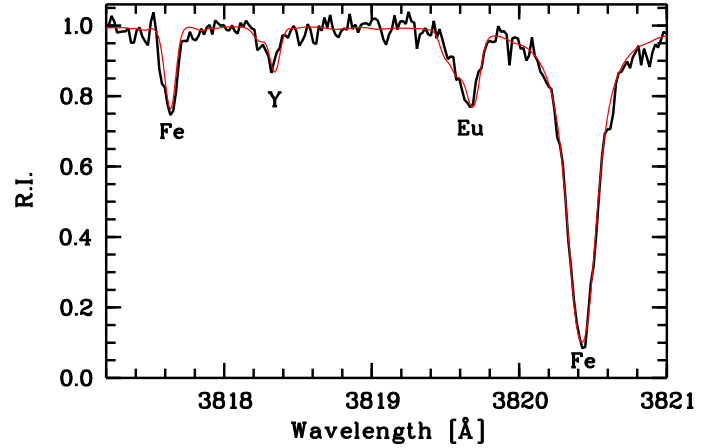


Fig. E.1. Residual intensity of the *Gaia* BH3 UVES spectrum (black line) compared with the modelled spectrum (thin red line) in the Eu region.

ment with the value derived from the SOPHIE spectrum ([Fe/H] = -2.57 ± 0.12 from 121 Fe I lines) and from the HERMES spectrum ([Fe/H] = -2.54 ± 0.14 from 156 Fe I lines). A good agreement was also obtained for the other elements, whose abundance is based on several lines. The star, as expected for the metal-poor regime, is enhanced in α elements.

There is no trace of ^{13}C in the spectrum, so the star has not been enriched by material processed in the CNO cycle, as it would if it had, for instance, accreted material from a companion star in the AGB phase.

The star has no chemical peculiarity, except a slight enhancement in Eu: [Eu/Fe] = 0.52. When coupled with [Ba/Fe] = 0.11, this classifies this star as an r-I neutron-capture-rich star, following the classification of Beers & Christlieb (2005). The UVES spectrum in the region of the Eu is shown in Fig. E.1.

According to the stellar parameters, the star is expected to have a Li abundance on the Mucciarelli plateau (see Mucciarelli et al. 2012). At the wavelength of the Li feature at 607 nm, we see an absorption line compatible with an abundance of $A(\text{Li}) = 1.2$, but the shape is not comparable with the synthetic spectrum, showing an absorption on the blue side of the feature. The Li feature is also visible in the SOPHIE spectrum, but with a lower S/N than in the UVES spectrum, while the S/N of the HERMES spectrum at 760 nm is too low.

Appendix F: Acknowledgements

This work presents results from the European Space Agency (ESA) space mission *Gaia*. *Gaia* data are being processed by the *Gaia* Data Processing and Analysis Consortium (DPAC). Funding for the DPAC is provided by national institutions, in particular the institutions participating in the *Gaia* MultiLateral Agreement (MLA). The *Gaia* mission website is <https://www.cosmos.esa.int/gaia>. The *Gaia* archive website is <https://archives.esac.esa.int/gaia>.

The *Gaia* mission and data processing have financially been supported by, in alphabetical order by country:

- the Algerian Centre de Recherche en Astronomie, Astrophysique et Géophysique of Bouzareah Observatory;
- the Australian Research Council (ARC) through an Australian Laureate Fellowship (awarded to Prof. Joss Bland-Hawthorn);

- the Austrian Fonds zur Förderung der wissenschaftlichen Forschung (FWF) Hertha Firnberg Programme through grants T359, P20046, and P23737;
- the BELgian federal Science Policy Office (BELSPO) for the provision of financial support in the framework of the PRODEX Programme of the European Space Agency (ESA), the Research Foundation Flanders (Fonds Wetenschappelijk Onderzoek) through grant VS.091.16N, the Fonds de la Recherche Scientifique (FNRS), and the Research Council of Katholieke Universiteit (KU) Leuven through grant C16/18/005 (Pushing AsteRoseismology to the next level with TESS, Gaia, and the Sloan Digital Sky Survey – PARADISE);
- the Brazil-France exchange programmes Fundação de Amparo à Pesquisa do Estado de São Paulo (FAPESP) and Coordenação de Aperfeiçoamento de Pessoal de Nível Superior (CAPES) - Comité Français d’Evaluation de la Coopération Universitaire et Scientifique avec le Brésil (COFECUB);
- the Chilean Agencia Nacional de Investigación y Desarrollo (ANID) through Fondo Nacional de Desarrollo Científico y Tecnológico (FONDECYT) Regular Project 1210992 (L. Chemin);
- the National Natural Science Foundation of China (NSFC) through grants 11573054, 11703065, and 12173069, the China Scholarship Council through grant 201806040200, and the Natural Science Foundation of Shanghai through grant 21ZR1474100;
- the Tenure Track Pilot Programme of the Croatian Science Foundation and the École Polytechnique Fédérale de Lausanne and the project TTP-2018-07-1171 ‘Mining the Variable Sky’, with the funds of the Croatian-Swiss Research Programme;
- the Czech-Republic Ministry of Education, Youth, and Sports through grant LG 15010 and INTER-EXCELLENCE grant LTAUSA18093, and the Czech Space Office through ESA PECS contract 98058;
- the Danish Ministry of Science;
- the Estonian Ministry of Education and Research through grant IUT40-1;
- the European Commission’s Sixth Framework Programme through the European Leadership in Space Astrometry (ELSA) Marie Curie Research Training Network (MRTN-CT-2006-033481), through Marie Curie project PIOFGA-2009-255267 (Space AsteroSeismology & RR Lyrae stars, SAS-RRL), and through a Marie Curie Transfer-of-Knowledge (ToK) fellowship (MTKD-CT-2004-014188); the European Commission’s Seventh Framework Programme through grant FP7-606740 (FP7-SPACE-2013-1) for the *Gaia* European Network for Improved data User Services (GENIUS) and through grant 264895 for the *Gaia* Research for European Astronomy Training (GREAT-ITN) network;
- the European Cooperation in Science and Technology (COST) through COST Action CA18104 ‘Revealing the Milky Way with *Gaia* (MW-*Gaia*)’;
- the European Research Council (ERC) through grants 320360 (The *Gaia*-ESO Milky Way Survey), 647208 (Do intermediate-mass black holes exist?), 687378 (Small Bodies: Near and Far), 682115 (Using the Magellanic Clouds to Understand the Interaction of Galaxies), 695099 (A sub-percent distance scale from binaries and Cepheids – CepBin), 745617 (Our Galaxy at full HD – Gal-HD), 834148 (Accelerating Galactic Archeology), 895174 (The build-up and fate of self-gravitating systems in the Universe), 947660 (Measuring Hubble’s Constant to 1% with Pulsating Stars – HIPStars), 951549 (Sub-percent calibration of the extragalactic distance scale in the era of big surveys – UniVerScale), 101004214 (Innovative Scientific Data Exploitation and Exploitation Applications for Space Sciences – EXPLORE), 101004719 (OPTICON-RadioNET Pilot), 101055318 (The 3D motion of the Interstellar Medium with ESO and ESA telescopes – ISM-FLOW), 101063193 (Evolutionary Mechanisms in the Milky way: the *Gaia* Data Release 3 revolution – EMMY), 101093572 (StarDance: the non-canonical evolution of stars in clusters) and 101135205 (HORIZON-CL4-2023-SPACE-01-71 SPACIOUS project);
- the European Science Foundation (ESF), in the framework of the *Gaia* Research for European Astronomy Training Research Network Programme (GREAT-ESF);
- the European Space Agency (ESA) in the framework of the *Gaia* project, through the Plan for European Cooperating States (PECS) programme through contracts C98090 and 4000106398/12/NL/KML for Hungary, through contract 4000115263/15/NL/IB for Germany, through Programme de Développement d’Expériences scientifiques (PRODEX) Experiment Arrangement grants 4000132054 for Hungary, 4000142234 (Inference of radial velocities from astrometric stellar data - ASTRO2RV) and 4000138941 (Gaia Astrometric Microlensing Events - GAME) for Slovenia and through contract 4000132226/20/ES/CM;
- the Research Council of Finland through grants 336546 and 345115 and Waldemar von Frenckells stiftelse;
- the French Centre National d’Études Spatiales (CNES), the Agence Nationale de la Recherche (ANR) through grant ANR-10-IDEX-0001-02 for the ‘Investissements d’avenir’ programme, through grant ANR-15-CE31-0007 for project ‘Modelling the Milky Way in the *Gaia* era’ (MOD4*Gaia*), through grant ANR-14-CE33-0014-01 for project ‘The Milky Way disc formation in the *Gaia* era’ (ARCHEOGAL), through grant ANR-15-CE31-0012-01 for project ‘Unlocking the potential of Cepheids as primary distance calibrators’ (UnlockCepheids), through grant ANR-19-CE31-0017 for project ‘Secular evolution of galaxies’ (SEGAL), and through grant ANR-18-CE31-0006 for project ‘Galactic Dark Matter’ (GaDaMa), the Centre National de la Recherche Scientifique (CNRS) and its SNO *Gaia* of the Institut des Sciences de l’Univers (INSU), its Programmes Nationaux: Cosmologie et Galaxies (PNCG), Gravitation Références Astronomie Métrologie (PNGRAM), Planétologie (PNP), Physique et Chimie du Milieu Interstellaire (PCMI), and Physique Stellaire (PNPS), supported by INSU along with the Institut National de Physique (INP) and the Institut National de Physique nucléaire et de Physique des Particules (IN2P3), and co-funded by CNES; the ‘Action Fédératrice *Gaia*’ of the Observatoire de Paris, and the Région de Franche-Comté;
- the German Aerospace Agency (Deutsches Zentrum für Luft- und Raumfahrt e.V., DLR) through grants 50QG0501, 50QG0601, 50QG0602, 50QG0701, 50QG0901, 50QG1001, 50QG1101, 50QG1401, 50QG1402, 50QG1403, 50QG1404, 50QG1904, 50QG2101, 50QG2102, and 50QG2202, and the Centre for Information Services and High Performance Computing (ZIH) at the Technische Universität Dresden for generous allocations of computer time;
- the Hungarian Academy of Sciences through the János Bolyai Research Scholarship (G. Marton and Z. Nagy) and the Hungarian National Research, Develop-

- ment, and Innovation Office (NKFIH) through grants KKP-137523 ('SeismoLab'), OTKA FK 146023 and TKP2021-NKTA-64;
- the Science Foundation Ireland (SFI) through a Royal Society - SFI University Research Fellowship (M. Fraser);
 - the Israel Ministry of Science and Technology through grant 3-18143 and the Israel Science Foundation (ISF) through grant 1404/22;
 - the Agenzia Spaziale Italiana (ASI) through contracts I/037/08/0, I/058/10/0, 2014-025-R.0, 2014-025-R.1.2015, and 2018-24-HH.0 and its addendum 2018-24-HH.1-2022 to the Italian Istituto Nazionale di Astrofisica (INAF), contract 2014-049-R.0/1/2, 2022-14-HH.0 to INAF for the Space Science Data Centre (SSDC, formerly known as the ASI Science Data Center, ASDC), contracts I/008/10/0, 2013/030/I.0, 2013-030-I.0.1-2015, and 2016-17-I.0 to the Aerospace Logistics Technology Engineering Company (ALTEC S.p.A.), INAF, and the Italian Ministry of Education, University, and Research (Ministero dell'Istruzione, dell'Università e della Ricerca) through the Premiale project 'Mining The Cosmos Big Data and Innovative Italian Technology for Frontier Astrophysics and Cosmology' (MITiC);
 - the Netherlands Organisation for Scientific Research (NWO) through grant NWO-M-614.061.414, through a VICI grant (A. Helmi), and through a Spinoza prize (A. Helmi), and the Netherlands Research School for Astronomy (NOVA);
 - the Polish National Science Centre through HARMONIA grant 2018/30/M/ST9/00311 and DAINA grant 2017/27/L/ST9/03221; the Ministry of Science and Higher Education (MNiSW) through grant DIR/WK/2018/12; the Polish National Agency for Academic Exchange through BEKKER fellowship BPN/BEK/2022/1/00106;
 - the Portuguese Fundação para a Ciência e a Tecnologia (FCT) through national funds, grants 2022.06962.PTDC and 2022.03993.PTDC, and work contract DL 57/2016/CP1364/CT0006, grants UIDB/04434/2020 and UIDP/04434/2020 for the Instituto de Astrofísica e Ciências do Espaço (IA), grants UIDB/00408/2020 and UIDP/00408/2020 for LASIGE, and grants UIDB/00099/2020 and UIDP/00099/2020 for the Centro de Astrofísica e Gravitação (CENTRA);
 - the Slovenian Research Agency through grants P1-0188, P1-0031, I0-0033, J1-8136, J1-2460 and N1-0344;
 - the Spanish Ministry of Economy (MINECO/FEDER, UE), the Spanish Ministry of Science and Innovation (MCIN), the Spanish Ministry of Education, Culture, and Sports, and the Spanish Government through grants BES-2016-078499, BES-2017-083126, BES-C-2017-0085, ESP2016-80079-C2-1-R, FPU16/03827, RTI2018-095076-B-C22, PID2021-122842OB-C22, PDC2021-121059-C22, and TIN2015-65316-P ('Computación de Altas Prestaciones VII'), the Juan de la Cierva Incorporación Programme (FJCI-2015-2671 and IJC2019-04862-I for F. Anders), the Severo Ochoa Centre of Excellence Programme (SEV2015-0493) and MCIN/AEI/10.13039/501100011033/EU FEDER and Next Generation EU/PRTR (PRTR-C17.I1 and CNS2022-135232); the European Union through European Regional Development Fund 'A way of making Europe' through grants PID2021-122842OB-C21 and PID2021-125451NA-I00, the Institute of Cosmos Sciences University of Barcelona (ICCUB, Unidad de Excelencia 'María de Maeztu') through grant CEX2019-000918-M, the University of Barcelona's official doctoral programme for the development of an R+D+i project through an Ajuts de Personal Investigador en Formació (APIF) grant, the [Spanish Virtual Observatory](#) project funded by MCIN/AEI/10.13039/501100011033/ through grant PID2020-112949GB-I00; the Centro de Investigación en Tecnologías de la Información y las Comunicaciones (CITIC), funded by the Xunta de Galicia through the collaboration agreement to reinforce CIGUS research centers, research consolidation grant ED431B 2021/36 and scholarships from Xunta de Galicia and the EU - ESF ED481A-2019/155 and ED481A 2021/296; the Red Española de Supercomputación (RES) computer resources at MareNostrum, the Barcelona Supercomputing Centre - Centro Nacional de Supercomputación (BSC-CNS) through activities AECT-2017-2-0002, AECT-2017-3-0006, AECT-2018-1-0017, AECT-2018-2-0013, AECT-2018-3-0011, AECT-2019-1-0010, AECT-2019-2-0014, AECT-2019-3-0003, AECT-2020-1-0004, and DATA-2020-1-0010, the Departament d'Innovació, Universitats i Empresa de la Generalitat de Catalunya through grant 2014-SGR-1051 for project 'Models de Programació i Entorns d'Execució Parallels' (MPEXPAN), and Ramon y Cajal Fellowships RYC2018-025968-I, RYC2021-031683-I and RYC2021-033762-I, funded by MICIN/AEI/10.13039/501100011033 and by the European Union NextGenerationEU/PRTR and the European Science Foundation ('Investing in your future'); the Port d'Informació Científica (PIC), through a collaboration between the Centro de Investigaciones Energéticas, Medioambientales y Tecnológicas (CIEMAT) and the Institut de Física d'Altes Energies (IFAE), supported by the grant EQC2021-007479-P funded by MCIN/AEI/ 10.13039/501100011033 and by the "European Union NextGenerationEU/PRTR), and also by MICIIN with funding from European Union NextGenerationEU(PRTR-C17.I1) and by Generalitat de Catalunya;
 - the Swedish National Space Agency (SNSA/Rymdstyrelsen);
 - the Swiss State Secretariat for Education, Research, and Innovation through the Swiss Activités Nationales Complémentaires and the Swiss National Science Foundation through an Eccellenza Professorial Fellowship (award PCEFP2_194638 for R.I. Anderson) and in the framework of the National Centre of Competence in Research PlanetS under grants 51NF40_182901 and 51NF40_205606;
 - the United Kingdom Particle Physics and Astronomy Research Council (PPARC), the United Kingdom Science and Technology Facilities Council (STFC), and the United Kingdom Space Agency (UKSA) through the following grants to the University of Bristol, Brunel University London, the Open University, the University of Cambridge, the University of Edinburgh, the University of Hertfordshire, the University of Leicester, the Mullard Space Sciences Laboratory of University College London, and the United Kingdom Rutherford Appleton Laboratory (RAL): PP/D006503/1, PP/D006511/1, PP/D006546/1, PP/D006570/1, PP/D006791/1, ST/I000852/1, ST/J005045/1, ST/K00056X/1, ST/K000209/1, ST/K000756/1, ST/K000578/1, ST/L002388/1, ST/L006553/1, ST/L006561/1, ST/N000595/1, ST/N000641/1, ST/N000978/1, ST/N001117/1, ST/S000089/1, ST/S000976/1, ST/S000984/1, ST/S001123/1, ST/S001948/1, ST/S001980/1, ST/S002103/1, ST/V000624/1, ST/V000969/1, EP/V520342/1, ST/W002469/1, ST/W002493/1, ST/W002671/1, ST/W002809/1, ST/W507490/1,

ST/X00158X/1, ST/X001601/1, ST/X001636/1, ST/X001687/1, ST/X002667/1, ST/X002683/1 and ST/X002969/1.

The *Gaia* project and data processing have made use of:

- the Set of Identifications, Measurements, and Bibliography for Astronomical Data (SIMBAD, [Wenger et al. 2000](#)), the ‘Aladin sky atlas’ ([Bonnarel et al. 2000](#); [Boch & Fernique 2014](#)), and the VizieR catalogue access tool ([Ochsenbein et al. 2000](#)), all operated at the Centre de Données astronomiques de Strasbourg (CDS);
- the National Aeronautics and Space Administration (NASA) Astrophysics Data System (ADS);
- the SPace ENVironment Information System (SPENVIS), initiated by the Space Environment and Effects Section (TEC-EES) of ESA and developed by the Belgian Institute for Space Aeronomy (BIRA-IASB) under ESA contract through ESA’s General Support Technologies Programme (GSTP), administered by the BELgian federal Science Policy Office (BELSPO);
- the software products TOPCAT, STIL, and STILTS ([Taylor 2005, 2006](#));
- Matplotlib ([Hunter 2007](#));
- IPython ([Pérez & Granger 2007](#));
- Astropy, a community-developed core Python package for Astronomy ([Astropy Collaboration et al. 2018](#));
- R (R Core Team 2013);
- the HEALPix package ([Górski et al. 2005](#), <http://healpix.sourceforge.net/>);
- Vaex ([Breddels & Veljanoski 2018](#));
- the HIPPARCOS-2 catalogue ([van Leeuwen 2007](#)). The HIPPARCOS and *Tycho* catalogues were constructed under the responsibility of large scientific teams collaborating with ESA. The Consortia Leaders were Lennart Lindgren (Lund, Sweden: NDAC) and Jean Kovalevsky (Grasse, France: FAST), together responsible for the HIPPARCOS Catalogue; Erik Høg (Copenhagen, Denmark: TDAC) responsible for the *Tycho* Catalogue; and Catherine Turon (Meudon, France: INCA) responsible for the HIPPARCOS Input Catalogue (HIC);
- the *Tycho-2* catalogue ([Høg et al. 2000](#)), the construction of which was supported by the Velux Foundation of 1981 and the Danish Space Board;
- the *Tycho* double star catalogue (TDSC, [Fabricius et al. 2002](#)), based on observations made with the ESA HIPPARCOS astrometry satellite, as supported by the Danish Space Board and the United States Naval Observatory through their double-star programme;
- data products from the Two Micron All Sky Survey (2MASS, [Skrutskie et al. 2006](#)), which is a joint project of the University of Massachusetts and the Infrared Processing and Analysis Center (IPAC) / California Institute of Technology, funded by the National Aeronautics and Space Administration (NASA) and the National Science Foundation (NSF) of the USA;
- the ninth data release of the AAVSO Photometric All-Sky Survey (APASS, [Henden et al. 2016](#)), funded by the Robert Martin Ayers Sciences Fund;
- the first data release of the Pan-STARRS survey ([Chambers et al. 2016](#); [Magnier et al. 2020a](#); [Waters et al. 2020](#); [Magnier et al. 2020c,b](#); [Flewelling et al. 2020](#)). The Pan-STARRS1 Surveys (PS1) and the PS1 public science archive have been made possible through contributions by the Institute for Astronomy, the University of Hawaii, the Pan-STARRS Project Office, the Max-Planck Society and its participating institutes, the Max Planck Institute for Astronomy, Heidelberg and the Max Planck Institute for Extraterrestrial Physics, Garching, The Johns Hopkins University, Durham University, the University of Edinburgh, the Queen’s University Belfast, the Harvard-Smithsonian Center for Astrophysics, the Las Cumbres Observatory Global Telescope Network Incorporated, the National Central University of Taiwan, the Space Telescope Science Institute, the National Aeronautics and Space Administration (NASA) through grant NNX08AR22G issued through the Planetary Science Division of the NASA Science Mission Directorate, the National Science Foundation through grant AST-1238877, the University of Maryland, Eotvos Lorand University (ELTE), the Los Alamos National Laboratory, and the Gordon and Betty Moore Foundation;
- the second release of the Guide Star Catalogue (GSC2.3, [Lasker et al. 2008](#)). The Guide Star Catalogue II is a joint project of the Space Telescope Science Institute (STScI) and the Osservatorio Astrofisico di Torino (OATo). STScI is operated by the Association of Universities for Research in Astronomy (AURA), for the National Aeronautics and Space Administration (NASA) under contract NAS5-26555. OATo is operated by the Italian National Institute for Astrophysics (INAF). Additional support was provided by the European Southern Observatory (ESO), the Space Telescope European Coordinating Facility (STECF), the International GEMINI project, and the European Space Agency (ESA) Astrophysics Division (nowadays SCI-S);
- the eXtended, Large (XL) version of the catalogue of Positions and Proper Motions (PPM-XL, [Roesser et al. 2010](#));
- data products from the Wide-field Infrared Survey Explorer (WISE), which is a joint project of the University of California, Los Angeles, and the Jet Propulsion Laboratory/California Institute of Technology, and NEOWISE, which is a project of the Jet Propulsion Laboratory/California Institute of Technology. WISE and NEOWISE are funded by the National Aeronautics and Space Administration (NASA);
- the first data release of the United States Naval Observatory (USNO) Robotic Astrometric Telescope (URAT-1, [Zacharias et al. 2015](#));
- the fourth data release of the United States Naval Observatory (USNO) CCD Astrograph Catalogue (UCAC-4, [Zacharias et al. 2013](#));
- the sixth and final data release of the Radial Velocity Experiment (RAVE DR6, [Steinmetz et al. 2020a,b](#)). Funding for RAVE has been provided by the Leibniz Institute for Astrophysics Potsdam (AIP), the Australian Astronomical Observatory, the Australian National University, the Australian Research Council, the French National Research Agency, the German Research Foundation (SPP 1177 and SFB 881), the European Research Council (ERC-StG 240271 Galactic), the Istituto Nazionale di Astrofisica at Padova, the Johns Hopkins University, the National Science Foundation of the USA (AST-0908326), the W.M. Keck foundation, the Macquarie University, the Netherlands Research School for Astronomy, the Natural Sciences and Engineering Research Council of Canada, the Slovenian Research Agency, the Swiss National Science Foundation, the Science & Technology Facilities Council of the UK, Opticon, Strasbourg Observatory, and the Universities of Basel, Groningen, Heidelberg, and Sydney. The RAVE website is at <https://www.rave-survey.org/>;

- the first data release of the Large sky Area Multi-Object Fibre Spectroscopic Telescope (LAMOST DR1, [Luo et al. 2015](#));
 - the K2 Ecliptic Plane Input Catalogue (EPIC, [Huber et al. 2016](#));
 - the ninth data release of the Sloan Digital Sky Survey (SDSS DR9, [Ahn et al. 2012](#)). Funding for SDSS-III has been provided by the Alfred P. Sloan Foundation, the Participating Institutions, the National Science Foundation, and the United States Department of Energy Office of Science. The SDSS-III website is <http://www.sdss3.org/>. SDSS-III is managed by the Astrophysical Research Consortium for the Participating Institutions of the SDSS-III Collaboration including the University of Arizona, the Brazilian Participation Group, Brookhaven National Laboratory, Carnegie Mellon University, University of Florida, the French Participation Group, the German Participation Group, Harvard University, the Instituto de Astrofísica de Canarias, the Michigan State/Notre Dame/JINA Participation Group, Johns Hopkins University, Lawrence Berkeley National Laboratory, Max Planck Institute for Astrophysics, Max Planck Institute for Extraterrestrial Physics, New Mexico State University, New York University, Ohio State University, Pennsylvania State University, University of Portsmouth, Princeton University, the Spanish Participation Group, University of Tokyo, University of Utah, Vanderbilt University, University of Virginia, University of Washington, and Yale University;
 - the thirteenth release of the Sloan Digital Sky Survey (SDSS DR13, [Albareti et al. 2017](#)). Funding for SDSS-IV has been provided by the Alfred P. Sloan Foundation, the United States Department of Energy Office of Science, and the Participating Institutions. SDSS-IV acknowledges support and resources from the Center for High-Performance Computing at the University of Utah. The SDSS web site is <https://www.sdss.org/>. SDSS-IV is managed by the Astrophysical Research Consortium for the Participating Institutions of the SDSS Collaboration including the Brazilian Participation Group, the Carnegie Institution for Science, Carnegie Mellon University, the Chilean Participation Group, the French Participation Group, Harvard-Smithsonian Center for Astrophysics, Instituto de Astrofísica de Canarias, The Johns Hopkins University, Kavli Institute for the Physics and Mathematics of the Universe (IPMU) / University of Tokyo, the Korean Participation Group, Lawrence Berkeley National Laboratory, Leibniz Institut für Astrophysik Potsdam (AIP), Max-Planck-Institut für Astronomie (MPIA Heidelberg), Max-Planck-Institut für Astrophysik (MPA Garching), Max-Planck-Institut für Extraterrestrische Physik (MPE), National Astronomical Observatories of China, New Mexico State University, New York University, University of Notre Dame, Observatório Nacional / MCTI, The Ohio State University, Pennsylvania State University, Shanghai Astronomical Observatory, United Kingdom Participation Group, Universidad Nacional Autónoma de México, University of Arizona, University of Colorado Boulder, University of Oxford, University of Portsmouth, University of Utah, University of Virginia, University of Washington, University of Wisconsin, Vanderbilt University, and Yale University;
 - the second release of the SkyMapper catalogue (SkyMapper DR2, [Onken et al. 2019](#), Digital Object Identifier 10.25914/5ce60d31ce759). The national facility capability for SkyMapper has been funded through grant LE130100104 from the Australian Research Council (ARC) Linkage Infrastructure, Equipment, and Facilities (LIEF) programme, awarded to the University of Sydney, the Australian National University, Swinburne University of Technology, the University of Queensland, the University of Western Australia, the University of Melbourne, Curtin University of Technology, Monash University, and the Australian Astronomical Observatory. SkyMapper is owned and operated by The Australian National University’s Research School of Astronomy and Astrophysics. The survey data were processed and provided by the SkyMapper Team at the Australian National University. The SkyMapper node of the All-Sky Virtual Observatory (ASVO) is hosted at the National Computational Infrastructure (NCI). Development and support the SkyMapper node of the ASVO has been funded in part by Astronomy Australia Limited (AAL) and the Australian Government through the Commonwealth’s Education Investment Fund (EIF) and National Collaborative Research Infrastructure Strategy (NCRIS), particularly the National eResearch Collaboration Tools and Resources (NeCTAR) and the Australian National Data Service Projects (ANDS);
 - the *Gaia*-ESO Public Spectroscopic Survey (GES, [Gilmore et al. 2022](#); [Randich et al. 2022](#)). The *Gaia*-ESO Survey is based on data products from observations made with ESO Telescopes at the La Silla Paranal Observatory under programme ID 188.B-3002. Public data releases are available through the [ESO Science Portal](#). The project has received funding from the Leverhulme Trust (project RPG-2012-541), the European Research Council (project ERC-2012-AdG 320360-*Gaia*-ESO-MW), and the Istituto Nazionale di Astrofisica, INAF (2012: CRA 1.05.01.09.16; 2013: CRA 1.05.06.02.07).
- The GBOT programme (**GBOT**) uses observations collected at (i) the European Organisation for Astronomical Research in the Southern Hemisphere (ESO) with the VLT Survey Telescope (VST), under ESO programmes 092.B-0165, 093.B-0236, 094.B-0181, 095.B-0046, 096.B-0162, 097.B-0304, 098.B-0030, 099.B-0034, 0100.B-0131, 0101.B-0156, 0102.B-0174, 0103.B-0165, 0104.B-0081, 0106.20ZA.001 (Omega-Cam), 0106.20ZA.002 (FORS2), 0108.21YF; and under INAF programs 110.256C, 112.266Q; and (ii) the Liverpool Telescope, which is operated on the island of La Palma by Liverpool John Moores University in the Spanish Observatorio del Roque de los Muchachos of the Instituto de Astrofísica de Canarias with financial support from the United Kingdom Science and Technology Facilities Council, and (iii) telescopes of the Las Cumbres Observatory Global Telescope Network.
- In addition to the currently active DPAC (and ESA science) authors of the peer-reviewed papers accompanying *Gaia* DR3, there are large numbers of former DPAC members who made significant contributions to the (preparations of the) data processing. Among those are, in alphabetical order: Stephanie Accart, Christopher Agard, Juan José Aguado, Michaël Ajaj, Fernando Aldea-Montero, Alexandra Alecu, Bruno Alessi, Peter Allan, France Allard, Walter Allasia, Carlos Allende Prieto, Javier Álvarez Cid-Fuentes, Marco Antonio Álvarez, João Alves, Antonio Amorim, Kader Amsif, Alexandre Andrei, Antonino Angi, Guillem Anglada-Escudé, Erika Antiche, Sonia Antón, Bernardino Arcay, Clément Arnaudeau, Borja Arroyo Galende, Vladan Arsenijevic, Tri Astraatmadja, Rajesh Kumar Bachchan, Adrien Bangma, Carlos Barata, Domenico Barbato, Fabio Barblan, Paul Barklem, Mickael Batailler, Duncan Bates, Alexandre Baudesson-Stella, Mathias Beck, Luigi Bedin, Dan Beilis, Antonio Bello García, Vasily Belokurov, Philippe Bendjoya, Ángel Berihuete, Hans Bernstein[†], Olivier Bienaymé, Lionel Bigot, Albert Bijaoui, Louis Bil, Françoise

Billebaud, Nadejda Blagorodnova, Thierry Bloch, Klaas de Boer[†], Marco Bonfigli, Giuseppe Bono, Simon Borgniet, Raul Borrachero-Sanchez, François Bouchy, Steve Boudreault, Geraldine Bourda, Guy Boutonnet, Lorenzo Bramante, Pascal Branet, Maarten Breddels, Scott Brown, Pierre-Marie Brunet, Thomas Brüsemeister, Peter Bunclark[†], Roberto Buonanno, Alexandru Burlacu, Robert Butorafuchs, Joan Cambras, Heather Campbell, Sylvain Cannizzo, Christophe Carret, Manuel Carrillo, César Carrión, Pau Castro Sampol, Francisco Javier Casquero, Laurence Chaoul, Jonathan Charnas, Fabien Chéreau, Vincenzo Chiaramida Mathurin Chritin, Maria-Rosa Cioni, Uma Claddellas Sanjuan, Marcial Clotet, Gabriele Cocozza, Ross Collins, Gabriele Comoretto, Gabriele Contursi, Leonardo Corcione, Gráinne Costigan, Françoise Crifo, Alessandro Crisafi, Nick Cross, Jan Cuypers[†], Jean-Charles Damery, Anastasios Daperoglas, Eric Darmigny, Pedro David, Jonas Debosscher, Peter De Cat, Domitilla De Martino, Rafael De Souza, Enrique Del Pozo, Héctor Delgado, David Delhoume, Céline Delle Luche, Markus Demleitner, Léo Denglos, Sékou Diakite, Paola Di Matteo, Carla Domingues, Sandra Dos Anjos, Laurent Douchy, Petros Drazinos, Pierre Dubath, Javier Durán, Yifat Dzigan, Bengt Edvardsson, Deepak Eappachen, Sebastian Els, Arjen van Elteren, Kjell Eriksson, Pilar Esquej, Carolina von Essen, Wyn Evans, Guillaume Eynard Bontemps, Antonio Falcão, Martí Farràs Casas, Jacopo Federici, Luciana Federici, Fernando de Felice, Agnès Fienga, Krzysztof Findeisen, Christian Fischer, Florin Fodor, Yori Fournier, Frédéric Franke, Benoît Frezouls, Aidan Fries, Jan Fuchs, Flavio Fusi Pecci, Diego Fustes, Duncan Fyfe, Eva Gallardo, Silvia Galleti, Fernando García, Alberto García Gutiérrez, María García-Reinaldos, Daniele Gardiol, Nora Garralda Torres, Emilien Gaudin, Alvin Gavel, Marwan Gebran, Yoann Gérard, Nathalie Gerbier, Joris Gerssen, Miguel Gomes, Roy Gomel, Anita Gómez, Ana González-Marcos, Juan González-Núñez, Juan José González-Vidal, Eva Grebel, Michel Grenon, Björn Grieger, Eric Grux, Alain Gueguen, Pierre Guillout, Julie Guiraud, Andrés Gúrpide, Leanne Guy, Jean-Louis Halbwachs, Marcus Hauser, Aurelien Hees, Kevin Henares, Julien Heu, Albert Heyrovsky, Thomas Hilger, Nathan Himpens, Natalia Hładczuk, Wilfried Hofmann, Erik Høg, David Hogg, Andrew Holland, Greg Holland, Gordon Hopkinson[†], Claude Huc, Pablo Huijse, Jason Hunt, Brigitte Huynh, Arkadiusz Hypki, Giacinto Iannicola, Sergio Ibarria, Vilma Icardi, Laura Inno, Mike Irwin, Yago Isasi Parache, Javier Izquierdo, Maja Jabłońska, Thierry Jacq, Asif Jan, Anne-Marie Janotto, Kevin Jardine, Gérard Jasiewicz, Anne Jean-Antoine Piccolo, Laurent Jean-Rigaud, Isabelle Jégouzo-Giroux, Christian Jezequel, François Jocteur-Monrozier, Paula Jofré, Anthony Jonckheere, Peter Jonker, Áron Juhász, Francisc Julbe, Antonios Karampelas, Lea Karbevská, Ralf Keil, Adam Kewley, Dae-Won Kim, Peter Klagyivik, Jochen Klar, Jonas Klüter, Jens Knude, Angela Kochoska, Oleg Kochukhov, Katrien Kolenberg, Indrek Kolka, Pavel Koubsky, Janez Kos, Irina Kovalenko, Daniel Krefl, Maria Kudryashova, Ilya Kull, Alex Kutka, Frédéric Lacoste-Seris, Sylvain Lafosse, Valéry Lainey, Pascal Laizeau, Yannick Lasne, Antoni Latorre, Felix Lauwaert, Claudia Lavalley, Jean-Baptiste Lavigne, David Le Bouquin, Jean-François Le Champion, Isabelle Lecoœur-Taibi, Yann Le Fustec, Vassili Lemaitre, Helmut Lenhardt, Christophe Le Poncin-Lafitte, Frédéric Leroux, Thierry Levoir, Hans Lindstrøm, Tim Lister, Chao Liu, Mauro López Del Fresno, Davide Loreggia, Denise Lorenz, Cristina Luengo, Ian MacDonald, Marc Madaule, Pau Madrero Pardo, Tiago Magalhães Fernandes, Arrate Magdaleno Romeo, Kirill Makan, Valeri Makarov, Jean-Christophe Malapert, Sandrine Managau, Hervé Manche, Carmelo Manetta, Gregory Mantelet,

José Marcos, Miguel Marcos Santos, Federico Marocco, Gabor Marschalko, Mathieu Marseille, Christophe Martayan, Óscar Martínez-Rubi, Michele Martino, Paul Marty, Nicolas Mary, Davide Massari, Benjamin Massart, Gal Matijevič, Mohamed Meharga, Emmanuel Mercier, Maria Messineo, Frédéric Meynadier, Daniel Michalik, Anthony Michon, Shan Mignot, Hadi Minbashian, Bruno Miranda, László Molnár, Marco Molinaro, Giacomo Monari, Marc Moniez, Ángel Montero, Alain Montmory, Roger Mor, Thierry Morel, Stephan Morgenthaler, Angelo Mulone, Ulisse Munari, Daniel Muñoz, Cillian Murphy, Jérôme Narbonne, Gijs Nelemans, Anne-Thérèse Nguyen, Luciano Nicastro, Sara Nieto, Thomas Nordlander, Alexandre Nouvel, Louis Noval, Markus Nullmeier, Derek O'Callaghan, Francisco Ocaña, Pierre Ocvirk, Alex Ogden, Joaquín Ordieres-Meré, Diego Ordóñez, Giuseppe Orrù, Patricio Ortiz, José Osinde, Jose Osorio, Dagmara Oszkiewicz, Alex Ouzounis, Hugo Palacin, Max Palmer, Aviad Panahi, Chantal Panem, Vincent Papy, Peregrine Park, Ester Pasquato, Xavier Passot, Stefan Payne-Wardenaar, Louis Pegoraro, Roselyne Pedrosa, Christian Peltzer, Hanna Pentikäinen, Xavier Peñalosa Esteller, Jordi Peralta, Rubén Pérez, Jean-Marc Petit, Fabien Péturaud, Bernard Pichon, Tuomo Pieniluoma, Anna Marina Piersimoni, François-Xavier Pineau, Enrico Pigozzi, Federic Pireddu, Bertrand Plez, Joel Poels[†], Aurelian Polidoro, Eric Poujoulet, Arnaud Poulain, Guylaine Prat, Thibaut Prod'homme, Andrej Prša, Elena Racero, Adrien Raffy, Silvia Ragaini, Serena Rago, Nicolas Rambaux, Piero Ranalli, Gregor Rauw, Andrew Read, José Rebordao, Philippe Redon, Rita Ribeiro, Ariadna Ribes Metidieri, Pascal Richard, Phil Richards, Carlos Ríos Díaz, Daniel Risquez, Adrien Rivard, Clement Robin, Brigitte Rocca-Volmerange, Maroussia Roelens, Hervé Rogues, Laurent Rohrbasser, Nicolas de Roll, Julia Roquette, Siv Rosén, Frederic Royer, Stefano Rubele, Laura Ruiz Dern, Idoia Ruiz-Fuertes, Federico Russo, Jan Rybizki, Albert Sáez Núñez, Jesús Salgado, Eugenio Salguero, Nik Samaras, Paula Sánchez Gayet, Víctor Sánchez Giménez, Toni Santana, Helder Savietto, Maud Segol, Juan Carlos Segovia, Damien Segransan, Léa Sellahannadi, Didier Semeux, I-Chun Shih, Hassan Siddiqui, Lauri Siltala, André Silva, Helder Silva, Arturo Silvelo, Dimitris Sinachopoulos, Christos Siopis, Riccardo Smareglia, Kester Smith, Michael Soffel, Sergio Soria Nieto, Danuta Sosnowska, Alessandro Spagna, Maxime Spano, Lorenzo Spina, Ulrike Stampa, Craig Stephenson, Hristo Stoev, Vytautas Straižys, Frank Suess, Maria Süveges, Elza Szegedi-Elek, Francis Tâche, Jeff Tambouez, Guy Tauran, Dirk Terrell, David Terrett, Pierre Teyssandier, Stephan Theil, William Thuillot, Carola Tiede, Brandon Tingley, Krešimir Tisanić, Anastasia Titarenko, Jordi Torra[†], Scott Trager, Licia Troisi, Paraskevi Tsalmantza, David Tur, Stefano Uzzi, Mattia Vaccari, Frédéric Vachier, Emmanouil Vachlas, Marc Vaillant, Gaetano Valentini, Pau Vallès, Veronique Valette, Emmanuel van Dillen, Walter Van Hamme, Eric Van Hemelryck, Wouter van Reeve, Mihaly Varadi, Marco Vaschetto, Jovan Veljanoski, Lionel Veltz, Sjoert van Velzen, Teresa Via, Yves Viala, Jenni Virtanen, Antonio Volpicelli, Holger Voss, Viktor Votruba, Stelios Voutsinas, Jean-Marie Wallut, Gavin Walmsley, Olivier Wertz, Thomas Wevers, Rainer Wichmann, Mark Wilkinson, Abdullah Yoldas, Patrick Yvard, Petar Zečević, Tim de Zeeuw, Maruska Zerjal, Hourii Ziaepour, Claude Zurbach, and Sven Zschocke.

In addition to the DPAC consortium, past and present, there are numerous people, mostly in ESA and in industry, who have made or continue to make essential contributions to *Gaia*, for instance those employed in science and mission operations or in the design, manufacturing, integration, and testing of the space-

craft and its modules, subsystems, and units. Many of those will remain unnamed yet spent countless hours, occasionally during nights, weekends, and public holidays, in cold offices and dark clean rooms. At the risk of being incomplete, we specifically acknowledge, in alphabetical order, from Airbus DS (Toulouse): Alexandre Affre, Marie-Thérèse Aimé, Audrey Albert, Aurélien Albert-Aguilar, Jeanine Alloun-Etcheberry, Hania Aرسالane, Arnaud Arousseau, Denis Bassi, Franck Bayle, Bernard Bayol, Pierre-Luc Bazin, Emmanuelle Benninger, Philippe Bertrand, Jean-Bernard Biau, François Binter, Cédric Blanc, Eric Blonde, Patrick Bonzom, Bernard Bories, Jean-Jacques Bouisset, Joël Boyadjian, Isabelle Brault, Corinne Buge, Bertrand Calvel, Jean-Michel Camus, France Canton, Lionel Carminati, Michel Carrie, Didier Castel, Philippe Charvet, François Chassat, Fabrice Cherouat, Ludovic Chirouze, Michel Choquet, Claude Coatic, Emmanuel Collados, Philippe Corberand, Christelle Dauga, Robert Davancens, Catherine Deblock, Eric Decourbey, Charles Dekhtiar, Michel Delannoy, Michel Delgado, Damien Delmas, Emilie Demange, Victor Depeyre, Isabelle Desenclos, Christian Dio, Kevin Downes, Marie-Ange Duro, Eric Ecale, Omar Emam, Elizabeth Estrada, Coralie Falgayrac, Benjamin Farcot, Claude Faubert, Frédéric Faye, Sébastien Finana, Grégory Flandin, Loic Floury, Gilles Fongy, Michel Fruit, Florence Fusero, Christophe Gabilan, Jérémie Gaboriaud, Cyril Gallard, Damien Galy, Benjamin Gandon, Patrick Gareth, Eric Gelis, André Gellon, Laurent Georges, Philippe-Marie Gomez, José Goncalves, Frédéric Guedes, Vincent Guillemier, Thomas Guilpain, Stéphane Halbout, Marie Hanne, Grégory Hazera, Daniel Herbin, Tommy Hercher, Claude Hoarau le Papillon, Matthias Holz, Philippe Humbert, Sophie Jallade, Grégory Jonniaux, Frédéric Juillard, Philippe Jung, Charles Koeck, Marc Labaysse, René Laborde, Anouk Laborie, Jérôme Lacoste-Barutel, Baptiste Laynet, Virginie Le Gall, Julien L'Hermitte, Marc Le Roy, Christian Lebranchu, Didier Lebreton, Patrick Lelong, Jean-Luc Leon, Stephan Leppke, Franck Levallois, Philippe Lingot, Laurant Lobo, Didier Loche, Céline Lopez, Jean-Michel Loupias, Carlos Luque, Sébastien Maes, Bruno Mamdy, Denis Marchais, Alexandre Marson, Benjamin Massart, Rémi Mauriac, Philippe Mayo, Caroline Meisse, Hervé Mercereau, Olivier Michel, Florent Minaire, Xavier Moisson, David Monteiro, Denis Montperrus, Boris Niel, Cédric Papot, Jean-François Pasquier, Gareth Patrick, Pascal Paulet, Martin Peciaccia, Sylvie Peden, Sonia Penalva, Michel Pendaries, Philippe Peres, Grégory Personne, Dominique Pierot, Jean-Marc Pillot, Lydie Pinel, Fabien Piquemal, Vincent Poinsignon, Maxime Pomelec, André Porras, Pierre Pouny, Severin Provost, Sébastien Ramos, Fabienne Raux, Audrey Rehby, Florian Reuscher, Xavier Richard, Nicolas Riguét, Mickael Roche, Gilles Rougier, Bruno Rouzier, Stéphane Roy, Jean-Paul Ruffie, Frédéric Safa, Heloise Scheer, Claudie Serris, André Sobeczko, Jean-François Soucaille, Romain Suze, Philippe Taty, Théo Thomas, Pierre Thorat, Dominique Torcheux, Vincent Tortel, Damien Tourbez, Stéphane Touzeau, Didier Trantoul, Cyril Vétel, Jean-Axel Vatinel, Jean-Paul Vormus, and Marc Zanoni; from Airbus DS (Friedrichshafen): Jan Beck, Frank Blender, Volker Hashagen, Armin Hauser, Bastian Hell, Cosmas Heller, Matthias Holz, Heinz-Dieter Junginger, Klaus-Peter Koeble, Karin Pietroboni, Ulrich Rauscher, Rebekka Reichle, Florian Reuscher, Ariane Stephan, Christian Stierle, Riccardo Vascotto, Christian Hehr, Markus Schelkle, Rudi Kerner, Udo Schuhmacher, Peter Moeller, Rene Stritter, Jürgen Frank, Wolfram Beckert, Evelyn Walsler, Steffen Roetzer, Fritz Vogel, and Friedbert Zilly; from Airbus DS (Stevenage): Mohammed Ali, Bill Bental, David Bibby, Leisha Carratt, Veronica Carroll, Clive Catley, Patrick

Chapman, Christopher Chetwood, Alison Colegrove, Tom Colegrove, Andrew Davies, Denis Di Filippantonio, Andy Dyne, Alex Elliot, Omar Emam, Colin Farmer, Steve Farrington, Nick Francis, Albert Gilchrist, Brian Grainger, Yann Le Hiress, Vicky Hodges, Jonathan Holroyd, Haroon Hussain, Roger Jarvis, Lewis Jenner, Steve King, Chris Lloyd, Neil Kimbrey, Alessandro Martis, Bal Matharu, Karen May, Florent Minaire, Katherine Mills, James Myatt, Chris Nicholas, Paul Norridge, David Perkins, Michael Pieri, Matthew Pigg, Angelo Povolieri, Robert Purvinskis, Phil Robson, Julien Saliege, Satti Sangha, Paramjit Singh, John Standing, Dongyao Tan, Keith Thomas, Rosalind Warren, Andy Whitehouse, Robert Wilson, Hazel Wood, Steven Danes, Scott Englefield, Juan Flores-Watson, Chris Lord, Allan Parry, Juliet Morris, Nick Gregory, and Ian Mansell.

From ESA, in alphabetical order: Ricard Abello, Asier Abreu, Ivan Aksenov, Matthew Allen, Salim Ansari, Philippe Armbruster, Mari-Liis Aru, Alessandro Atzei, Liesse Ayache, Samy Azaz, Nana Bach, Jean-Pierre Balley, Paul Balm, Manuela Baroni, Rainer Bauske, Thomas Beck, Gabriele Bellei, Carlos Bielsa, Gerhard Billig, Carmen Blasco, Andreas Boosz, Bruno Bras, Julia Braun, Thierry Bru, Frank Budnik, Joe Bush, Marco Butkovic, Jacques Candéé, David Cano, Carlos Casas, Francesco Castellini, David Chapman, Nebil Cinar, Mark Clements, Giovanni Colangelo, Peter Collins, Ana Colorado McEvoy, Gabriele Comoretto, Vincente Companys, Federico Cordero, Yannis Croizat, Sylvain Damiani, Fabienne Delhaise, Gianpiero Di Girolamo, Yannis Diamantidis, John Dodsworth, Ernesto Dölling, Jane Douglas, Jean Doutreleau, Dominic Doyle, Mark Drapes, Frank Dreger, Peter Droll, Gerhard Drolshagen, Michal Ďurovič, Bret Durrett, Christina Eilers, Yannick Enginger, Alessandro Ercolani, Matthias Erdmann, Orcun Ergincan, Robert Ernst, Daniel Escolar, Maria Espina, Hugh Evans, Fabio Favata, Stefano Ferreri, Daniel Firre, Michael Flegel, Melanie Flentge, Alan Flowers, Steve Foley, Julia Fortuno-Benavent, Jens Freihöfer, Rob Furnell, Julio Gallegos, Maria De La Cruz Garcia Gonzalez, Philippe Garé, Wahida Gasti, José Gavira, Frank Geerling, Franck Germes, Gottlob Gienger, Bénédicte Girouart, Bernard Godard, Nick Godfrey, César Gómez Hernández, Roy Gouka, Cosimo Greco, Robert Guilanya, Kester Habermann, Manfred Hadwiger, Ian Harrison, Angela Head, Martin Hechler, Javier Hernandez Bravo, Kjeld Hjortnaes, John Hoar, Jacolien Hoek, Frank Hoffmann, Justin Howard, Fredrik Hülphers, Arjan Hulsbosch, Christopher Hunter, Premysl Janik, José Jiménez, Emmanuel Joliet, Helma van de Kamp-Glasbergen, Simon Kellest, Andrea Kerruish, Kevin Kewin, Oliver Kiddle, Sabine Kielbassa, Volker Kirschner, Kees van 't Klooster, Ralf Kohley, Jan Kolmas, Oliver El Korashy, Arek Kowalczyk, Holger Krag, Benoît Lainé, Markus Landgraf, Sven Landström, Mathias Lauer, Robert Launer, Laurence Tu-Mai Levan, Mark ter Linden, Santiago Llorente, Tim Lock[†], Alejandro Lopez-Lozano, Guillermo Lorenzo, Tiago Loureiro, James Madison, Juan Manuel Garcia, Federico di Marco, Jonas Marie, Filip Marinic, Pier Mario Besso, Arturo Martín Polegre, Ander Martínez, Monica Martínez Fernández, Marco Massaro, Paolo de Meo, Ana Mestre, Claudio Mevi, Luca Michienzi, David Milligan, Ali Mohammadzadeh, David Monteiro, Richard Morgan-Owen, Trevor Morley, Prisca Mühlmann, Jana Mulacova, Michael Müller, Pablo Muñoz, Petteri Nieminen, Alfred Nillies, Wilfried Nzoubou, Alistair O'Connell, Karen O'Flaherty, Alfonso Olias Sanz, William O'Mullane, José Osinde, Oscar Pace, Mohini Parameswaran, Ramon Pardo, Taniya Parikh, Paul Parsons, Panos Partheniou, Torgeir Paulsen, Dario Pellegrinetti, José-Louis Pellon-Bailon, Joe Pereira, Michael Perryman, Christian

Philippe, Alex Popescu, Frédéric Raison, Riccardo Rampini, Florian Renk, Alfonso Rivero, Andrew Robson, Gerd Rössling, Martina Rossmann, Markus Rückert, Andreas Rudolph, Frédéric Safa, Johannes Sahlmann, Eugenio Salguero, Jamie Salt, Giovanni Santin, Fabio de Santis, Rui Santos, Giuseppe Sarri, Stefano Scaglioni, Melanie Schabe, Dominic Schäfer, Micha Schmidt, Rudolf Schmidt, Ared Schnorhk, Klaus-Jürgen Schulz, Jean Schütz, Julia Schwartz, Andreas Scior, Jörg Seifert, Christopher Semprinoschnig[†], Ed Serpell, Iñaki Serraller Vizcaino, Gunther Sessler, Felicity Sheasby, Alex Short, Hassan Siddiqui, Heike Sillack, Swamy Siram, Chloe Sivac, Christopher Smith, Claudio Sollazzo, Steven Straw, Daniel Tapiador, Pilar de Teodoro, Mark Thompson, Giulio Tonelloto, Felice Torelli, Raffaele Tosellini, Cecil Tranquille, Irren Tsu-Silva, Livio Tucci, Aileen Urwin, Jean-Baptiste Valet, Martin Vannier,

Enrico Vassallo, David Verrier, Sam Verstaen, Rüdiger Vetter, José Villalvilla, Raffaele Vitulli, Mildred Vögele, Sandra Vogt, Sergio Volonté, Catherine Watson, Karsten Weber, Daniel Werner, Gary Whitehead[†], Gavin Williams, Alistair Winton, Michael Witting, Peter Wright, Karlie Yeung, Marco Zambianchi, and Igor Zayer, and finally Vincenzo Innocente from the Conseil Européen pour la Recherche Nucléaire (CERN).

In case of errors or omissions, please contact the [Gaia Helpdesk](#).

A.J. acknowledges support from the Fonds de la Recherche Fondamentale Collective (FNRS, F.R.F.C.) of Belgium through grant PDR T.0115.23 and from Belspo/PRODEX/ESA under grant PEA nr. 4000119826. This research made use of *pystrometry*, an open source Python package for astrometry timeseries analysis ([Sahlmann 2019](#)), and *galpy*, a Python library for Galactic dynamics ([Bovy 2015](#)).